

Functional Spatial Autoregressive Models

Tadao Hoshino*

October 2, 2024

Abstract

This study introduces a novel spatial autoregressive model in which the dependent variable is a function that may exhibit functional autocorrelation with the outcome functions of nearby units. This model can be characterized as a simultaneous integral equation system, which, in general, does not necessarily have a unique solution. For this issue, we provide a simple condition on the magnitude of the spatial interaction to ensure the uniqueness in data realization. For estimation, to account for the endogeneity caused by the spatial interaction, we propose a regularized two-stage least squares estimator based on a basis approximation for the functional parameter. The asymptotic properties of the estimator including the consistency and asymptotic normality are investigated under certain conditions. Additionally, we propose a simple Wald-type test for detecting the presence of spatial effects. As an empirical illustration, we apply the proposed model and method to analyze age distributions in Japanese cities.

arXiv:2402.14763v3 [econ.EM] 1 Oct 2024

*School of Political Science and Economics, Waseda University, 1-6-1 Nishi-waseda, Shinjuku-ku, Tokyo 169-8050, Japan. Email: thoshino@waseda.jp.

1 Introduction

Spatial interdependence among units is an essential element in spatial data analysis. To incorporate spatial interactions into econometric analysis, researchers have extensively utilized the Spatial Autoregressive (SAR) model:

$$y_i = \alpha_0 \sum_{j=1}^n w_{i,j} y_j + x_i^\top \beta_0 + \varepsilon_i, \quad (1.1)$$

where y_i denotes a scalar outcome, $w_{i,j}$ denotes a known *spatial weight* between i and j , x_i denotes a vector of explanatory variables, and ε_i denotes an error term. The *spatial lag* term $\sum_{j=1}^n w_{i,j} y_j$ captures the spatial trend of the outcome variable in the neighborhood of i , and the scalar parameter α_0 measures its impact. The usefulness of SAR modelling (1.1) has been demonstrated in various empirical topics, including regional economics, local politics, real estate, crimes, etc. In addition, if we define the weight term $w_{i,j}$ based on social distance or friendship connections instead of geographic distance, then the SAR models can be utilized to analyze social network data, and their applicability is vast.

To further broaden the applications of SAR modelling, this study aims to extend (1.1) to a functional SAR model where the dependent variable is a function defined on a common closed interval:

$$q_i(s) = \sum_{j=1}^n w_{i,j} \int_0^1 q_j(t) \alpha_0(t, s) dt + x_i^\top \beta_0(s) + \varepsilon_i(s), \quad \text{for } s \in [0, 1], \quad (1.2)$$

where $q_i : [0, 1] \rightarrow \mathbb{R}$ denotes the outcome function of interest. Restricting the support to $[0, 1]$ is a normalization. In particular, for empirical relevance, this study primarily focuses on the case in which q_i is the quantile function for a scalar dependent variable of interest. Regression models involving functional variables have been widely studied in the literature of functional data analysis (FDA) for several decades (e.g., [Ramsay and Silverman, 2005](#)). Our model is essentially different from the existing ones in that we explicitly consider the simultaneous spatial interactions of the outcome functions.

As a motivating example, suppose we intend to investigate the impact of a regional childcare subsidy program in a given city on the age distribution of the city. The policy is likely to attract households with young children from other regions to benefit from the subsidy. Additionally, if childcare facilities and schools need to be newly constructed, inflows of other age groups can also be anticipated as workers. To obtain a comprehensive picture of the shift in the age distribution owing to the subsidy program in its entirety, it would be natural to consider a regression model in which the dependent variable represents the age distribution of each city, such as the quantile function. Meanwhile, when the size of the young population in a given city is in an increasing trend (no matter the cause), which serves as a driver of economic growth of the city, this might also lead to an influx of working-age population into the surrounding regions owing to the spatial spillover of economic activities. The proposed functional SAR model (1.2) is able to account for such interdependency between the outcome functions of nearby spatial units.

In the literature, we are not the first to consider an SAR-type modelling in the functional regression context. [Zhu et al. \(2022\)](#) proposed a social network model similar to ours in a time-series setting,

where the response variable is a function of time. They assumed that only concurrent interactions exist at each moment such that the past and future outcomes of others do not affect the present outcome. Consequently, when fixed at each time point, their model can be reduced to the standard SAR model in (1.1). In this regard, our model may be considered to be a generalization of theirs such that $\alpha_0(t, s) \neq 0$ is allowed for $t \neq s$ in general.

Another related modelling approach to ours is the SAR quantile regression (e.g., [Su and Yang, 2011](#); [Malikov et al., 2019](#); [Ando et al., 2023](#)). When q_i represents a quantile function, our model and theirs are conceptually similar in that both approaches can examine the distributional effects of explanatory variables on the outcome and the spatial interaction of outcomes in a unified framework. However, a fundamental distinction lies in that we consider a model in which each unit has its own unique quantile function as the dependent variable. Consequently, we can explicitly allow for each specific quantile value of an outcome to interact with other quantiles of others' outcomes. For instance, our model can investigate the impacts of median outcome of neighborhoods on a specific (say) 10 percentile value of own outcome. In the time-series context, [Dong et al. \(2024\)](#) consider the same type of interaction structure as above.

Notice that our model (1.2) is characterized as a simultaneous integral equation system, and to the best of our knowledge, this type of modelling has not been investigated in the econometrics literature. To construct a consistent estimator for our model, the model space should be restricted such that the realized q_i 's are uniquely (in some sense) associated with the true parameters. We show that to establish this uniqueness property, as in the standard SAR model (cf. [Kelejian and Prucha, 2010](#)), the spatial effects α_0 must be bounded within a certain range. In particular, we demonstrate that the tightness of the bound required for α_0 depends on the smoothness of the outcome function.

To estimate the model parameters, we need to address the endogeneity issue arising from the simultaneous interaction among the outcome functions. Thus, we propose a regularized two-stage least squares (2SLS) estimator that is based on a series approximation of $\alpha_0(\cdot, s)$ at each evaluation point s . Under the availability of a sufficient number of instrumental variables (IVs) and regularity conditions, we prove that both the estimator for β_0 and that for $\alpha_0(t, s)$ are consistent at certain convergence rates and asymptotically normally distributed. Additionally, we develop a Wald-type test for assessing the presence of any spatial effects at each s . We show that the proposed test statistic asymptotically distributes as the standard normal after appropriate normalization. Furthermore, we discuss performing the estimation when the outcome functions are not fully observable on the entire interval $[0, 1]$, but are only discretely observed, which is typical in most empirical situations. Our proposed estimator relies on a simple interpolation method, and we derive a set of conditions under which the estimator can achieve the same asymptotic properties as the infeasible counterpart.

As an empirical illustration, we investigate the determinants of age distribution in Japanese cities. Since many Japanese cities are currently rapidly aging, which has emerged as one of the central social problems in the country, understanding the mechanisms underlying the age structure of cities is crucial. Using recent government survey data, including the Census, we apply our estimation and testing method to 1883 Japanese cities. Here, the outcome function q_i represents the quantile function of the age distribution in city i , and covariates x_i include variables such as annual commercial sales, unemployment rate, number of childcare facilities, and others. Our results suggest that spatial interaction effects are

extremely weak at quantiles close to the boundary points 0 or 1. This may not be surprising as all individuals are born at age 0 and have a life expectancy of approximately 100 years at maximum, resulting in little regional heterogeneity. In contrast, strong spatial effects are observed when both t and s are at approximately the ages of young working population, possibly indicating that economic activities and their spillovers are the main factors in shaping the spatial trend of age structure.

The remainder of this paper is organized as follows: In Section 2, we formally introduce the model proposed in this study and discuss the condition under which it is well defined with a unique solution. In addition, focusing on the cases where the outcome function is a quantile function, we discuss the motivations and interpretation of such a modelling approach. In Section 3, we describe our 2SLS method for estimating β_0 and α_0 . Thereafter, we study the asymptotic properties of the proposed estimator under a set of assumptions. In this section, we also propose a test statistic for testing the null hypothesis that $\alpha_0(t, s) = 0$ for $t \in \mathcal{I}$, and its asymptotic distribution is derived. In Section 4, we present the results of Monte Carlo experiments to evaluate the finite sample performance of the proposed estimator and test. Section 5 presents our empirical analysis on the age distribution of Japanese cities, and Section 6 concludes the paper.

Notation For a natural number n , I_n denotes an $n \times n$ identity matrix. For a function h defined on $[0, 1]$, the L^p norm of h is written as $\|h\|_{L^p} := (\int_0^1 |h(s)|^p ds)^{1/p}$, and $L^p(0, 1)$ denotes the set of h 's such that $\|h\|_{L^p} < \infty$. For a random variable x , the L^p norm of x is written as $\|x\|_p := (\mathbb{E}|x|^p)^{1/p}$. For a matrix A , $\|A\|$ and $\|A\|_\infty$ denote the Frobenius norm and the maximum absolute row sum of A , respectively. If A is a square matrix, we use $\rho_{\max}(A)$ and $\rho_{\min}(A)$ to denote its largest and smallest eigenvalues, respectively. In addition, A^- is a symmetric generalized inverse of A . We write $a \lesssim b$ and $a \lesssim_p b$ if $a = O(b)$ and $a = O_P(b)$, respectively. Finally, we write $a \sim b$ when $a \lesssim b$ and $b \lesssim a$.

2 Functional SAR Models

2.1 Model Setup and Completeness

Suppose that we have data of size n : $\{(q_i, x_i, w_{i,1}, \dots, w_{i,n})\}_{i=1}^n$, where q_i denotes a random outcome function of interest with the common support $[0, 1]$, $x_i = (x_{i,1}, \dots, x_{i,d_x})^\top \in \mathbb{R}^{d_x}$ denotes a vector of covariates including a constant term, and $w_{i,j} \in \mathbb{R}$ denotes the (i, j) -th element of an $n \times n$ pre-specified spatial weight matrix $W_n = (w_{i,j})_{i,j=1}^n$. The value of each $w_{i,j}$ is determined non-randomly. As is the convention, we set $w_{i,i} = 0$ for all i for normalization. Note that the spatial configurations of the units generally change with the sample size. Thus, the variables generally form triangular arrays, and model parameters depend on n through spatial interactions. However, when there is no confusion, the dependence on n is suppressed for notational convenience.

As shown in (1.2), our working model is

$$q_i(s) = \int_0^1 \bar{q}_i(t) \alpha_0(t, s) dt + x_i^\top \beta_0(s) + \varepsilon_i(s), \quad \text{for } s \in [0, 1],$$

where \bar{q}_i denotes the spatial lag of the outcome function: $\bar{q}_i := \sum_{j=1}^n w_{i,j} q_j$. The unknown parameters

to be estimated are α_0 and $\beta_0 = (\beta_{01}, \dots, \beta_{0d_x})^\top$. For instance, in our empirical analysis, $q_i(s)$ denotes the s -th quantile of the age distribution in city i , and $\alpha_0(t, s)$ captures the impacts from the t -th quantile ages of neighborhood cities to the s -th quantile age of own city. For other examples, $q_i(s)$ could be the s -th quantile of the income distribution in city i , s -th quantile of the daily activity energy expenditure of person i , number of available bicycles at the bicycle-sharing station i at time s , and so forth. Hereinafter, we assume that $q_i \in L^p(0, 1)$ for some $2 \leq p < \infty$ and that $\alpha_0 \in C[0, 1]^2$, where $C[0, 1]^2$ denotes the set of continuous functions on $[0, 1]^2$.

Before turning to the estimation of α_0 and β_0 , we discuss the *completeness* of our model, that is, whether model (1.2) can be characterized by a unique solution (q_1, \dots, q_n) . As our model comprises a system of n functional equations, the existence and uniqueness of the solution are non-trivial problems. If the system does not have or has multiple solutions, consistently estimating the model parameters without some ad hoc assumptions is generally impossible.

Let $Q(s) = (q_1(s), \dots, q_n(s))^\top$, $X = (x_1, \dots, x_n)^\top$, and $\mathcal{E}(s) = (\varepsilon_1(s), \dots, \varepsilon_n(s))^\top$. Then, we can re-write (1.2) in matrix form as

$$Q(s) = W_n \int_0^1 Q(t) \alpha_0(t, s) dt + X \beta_0(s) + \mathcal{E}(s).$$

This expression suggests that our model is seen as a system of *Fredholm integral equations of the second kind* with kernel $\alpha_0(t, s)$. Defining $\bar{\alpha}_0 := \max_{(t,s) \in [0,1]^2} |\alpha_0(t, s)|$, whose existence is ensured under the continuity of α_0 , assume the following:

Assumption 2.1. $\bar{\alpha}_0 \lesssim 1$ and $\|W_n\|_\infty \lesssim 1$ such that $\bar{\alpha}_0 \|W_n\|_\infty < 1$.

Let us denote $\mathcal{H}_{n,p} := \{H = (h_1, \dots, h_n) : h_i \in L^p(0, 1) \text{ for all } i\}$, and define a linear operator \mathcal{T} as

$$(\mathcal{T}H)(s) := W_n \int_0^1 H(t) \alpha_0(t, s) dt, \text{ for } H \in \mathcal{H}_{n,p},$$

whose range is $\mathcal{H}_{n,p}$ under Assumption 2.1. Thus, we can write $Q = \mathcal{T}Q + X\beta_0 + \mathcal{E}$. Then, denoting Id to be the identity operator, if the inverse operator $(\text{Id} - \mathcal{T})^{-1}$ exists, the solution Q of the system can be uniquely determined (as an element of $\mathcal{H}_{n,p}$) as $Q = (\text{Id} - \mathcal{T})^{-1}[X\beta_0 + \mathcal{E}]$.

The next proposition states that Assumption 2.1 is sufficient for the existence of $(\text{Id} - \mathcal{T})^{-1}$ and uniqueness of Q .

Proposition 2.1. Suppose that Assumption 2.1 holds. Then, $(\text{Id} - \mathcal{T})^{-1}$ exists, and Q is the only solution of (1.2) in the Banach space $(\mathcal{H}_{n,p}, \|\cdot\|_{\infty,p})$, where $\|H\|_{\infty,p} := \max_{1 \leq i \leq n} \|h_i\|_{L^p}$.

The proof is straightforward. Under Assumption 2.1, we have

$$\begin{aligned} \|\{\mathcal{T}H\}_i\|_{L^p} &= \left\| \sum_{j=1}^n w_{i,j} \int_0^1 h_j(t) \alpha_0(t, \cdot) dt \right\|_{L^p} \leq \sum_{j=1}^n |w_{i,j}| \left(\int_0^1 \left| \int_0^1 h_j(t) \alpha_0(t, s) dt \right|^p ds \right)^{1/p} \\ &\leq \sum_{j=1}^n |w_{i,j}| \left(\int_0^1 \int_0^1 |h_j(t)|^p |\alpha_0(t, s)|^p dt ds \right)^{1/p} \quad (2.1) \\ &\leq \bar{\alpha}_0 \|W_n\|_\infty \max_{1 \leq j \leq n} \|h_j\|_{L^p} < \|H\|_{\infty,p} < \infty \end{aligned}$$

for any $H \in \mathcal{H}_{n,p}$ by Minkowski's and Jensen's inequalities. This implies that $\mathcal{T}H \in \mathcal{H}_{n,p}$. As is well known, if the operator norm of \mathcal{T} is smaller than one, $(\text{Id} - \mathcal{T})^{-1}$ exists, and we have the Neumann series expansion $(\text{Id} - \mathcal{T})^{-1} = \sum_{\ell=0}^{\infty} \mathcal{T}^{\ell}$ converging in the operator norm (e.g., Theorem 2.14, [Kress \(2014\)](#)). It is immediate from (2.1) that $\|\mathcal{T}H\|_{\infty,p} < 1$ follows for any H such that $\|H\|_{\infty,p} = 1$, which yields the desired result.

When the spatial weight matrix is row-normalized such that $\|W_n\|_{\infty} = 1$, as is often the case in empirical applications, Assumption 2.1 can be reduced to $\bar{\alpha}_0 < 1$, which somewhat resembles the solvability condition $|\alpha_0| < 1$ for the standard linear SAR model (1.1).

Remark 2.1 (Alternative condition). If one imposes a stronger assumption on the space of the input functions, the requirement for the kernel can be relaxed. For example, for all i , suppose that q_i belongs to $C[0, 1]$. Then, by the extreme value theorem, q_i 's are bounded. Letting $\mathcal{H}_{n,\infty} := \{H = (h_1, \dots, h_n) : h_i \in C[0, 1] \text{ for all } i\}$ and $\|H\|_{\infty,\infty} := \max_{1 \leq i \leq n} \max_{s \in [0,1]} |h_i(s)|$, we can easily show that Q is the only solution in the Banach space $(\mathcal{H}_{n,\infty}, \|\cdot\|_{\infty,\infty})$ if $\|W_n\|_{\infty} \max_{s \in [0,1]} \int_0^1 |\alpha_0(t, s)| dt < 1$ is satisfied.¹ If the spatial weight matrix is row-normalized, then the condition can be further simplified to $\max_{s \in [0,1]} \int_0^1 |\alpha_0(t, s)| dt < 1$, which is a familiar requirement for the solvability of the Fredholm integral equation of the second kind (e.g., Corollary 2.16, [Kress \(2014\)](#)). It is known that compactly supported continuous functions are dense in L^p ($1 \leq p < \infty$). Thus, in practice, assuming that all q_i 's are continuous is almost harmless, and hence the violation of Assumption 2.1 should be allowed to some extent.

The Neumann series expansion implies that Q can be expressed as $Q = X\beta_0 + \mathcal{T}X\beta_0 + \mathcal{T}^2X\beta_0 + \dots + \mathcal{E} + \mathcal{T}\mathcal{E} + \mathcal{T}^2\mathcal{E} + \dots$, that is,

$$Q(\cdot) = X\beta_0(\cdot) + W_n X \int_0^1 \beta_0(t) \alpha_0(t, \cdot) dt + W_n W_n X \int_0^1 \int_0^1 \beta_0(t_1) \alpha_0(t_1, t_2) \alpha_0(t_2, \cdot) dt_1 dt_2 + \dots$$

Hence, the marginal effect of increasing $x_{i,j}$ on $Q(\cdot)$ is obtained by

$$\frac{\partial Q(\cdot)}{\partial x_{i,j}} = \mathbf{e}_i \beta_{0j}(\cdot) + W_n \mathbf{e}_i \int_0^1 \beta_{0j}(t) \alpha_0(t, \cdot) dt + W_n W_n \mathbf{e}_i \int_0^1 \int_0^1 \beta_{0j}(t_1) \alpha_0(t_1, t_2) \alpha_0(t_2, \cdot) dt_1 dt_2 + \dots,$$

where \mathbf{e}_i denotes the i -th column of I_n . This clearly shows that a change in i 's covariate affects not only the outcome of i but also those of other units through the spatial interaction - the so-called *spatial multiplier* effect.

2.2 Leading Example: A Distributional SAR Model

One of the situations in which model (1.2) can be most nicely applied empirically would be when the outcome function q_i represents the quantile function for the cumulative distribution function (CDF) of

¹Clearly, for any given $H \in \mathcal{H}_{n,\infty}$ such that $\|H\|_{\infty,\infty} = 1$, we have

$$|\{(\mathcal{T}H)(s)\}_i| \leq \sum_{j=1}^n |w_{i,j}| \int_0^1 |h_j(t)| \cdot |\alpha_0(t, s)| dt \leq \|W_n\|_{\infty} \max_{s \in [0,1]} \int_0^1 |\alpha_0(t, s)| dt.$$

a variable of interest. In our empirical analysis, we study the determinants of the *population pyramids* of Japanese cities by employing the age quantile function of city i as q_i .

Suppose that for each i we can observe a random CDF F_i for an outcome variable $y \in \mathcal{Y}_i \subseteq \mathbb{R}$ of interest. The quantile function of y for i is defined as $q_i(s) := \inf\{y \in \mathcal{Y}_i : s \leq F_i(y)\}$. In the FDA literature, models where the response variable represents a probability distribution have garnered significant attention, for example, [Petersen and Müller \(2016\)](#), [Han et al. \(2020\)](#), [Yang et al. \(2020\)](#), [Yang \(2020\)](#), [Ghodrati and Panaretos \(2022\)](#), [Petersen et al. \(2021\)](#), [Chen et al. \(2023\)](#). For an excellent review on this topic, refer to [Petersen et al. \(2022\)](#). A common view in these studies is that performing a regression analysis directly in the space of CDFs (or densities) is often problematic. Hence, we should consider imposing a regression model on the quantile function (rather than on the CDF per se), as in [Yang et al. \(2020\)](#) and [Yang \(2020\)](#), enabling us to enjoy several analytically and interpretationally preferable properties as mentioned below.

First, quantile functions can be easily computed without considering the range boundaries, unlike CDFs. Second, the domains of CDFs are typically heterogeneous across individuals, whereas that of quantile functions is always the fixed interval $[0, 1]$. Third, the least-squares regression of the quantile function can be nicely interpreted as a *Wasserstein distance* minimization problem.

More specifically for the third point, denoting $F_i^{\alpha, \beta}$ to be the CDF induced from the quantile function $q_i^{\alpha, \beta}(s) := \int_0^1 \bar{q}_i(t) \alpha(t, s) dt + x_i^\top \beta(s)$, the squared 2-Wasserstein distance between F_i and $F_i^{\alpha, \beta}$ is obtained as²

$$\mathcal{W}_2^2(F_i, F_i^{\alpha, \beta}) = \int_0^1 \left(q_i(s) - q_i^{\alpha, \beta}(s) \right)^2 ds.$$

Thus, minimizing the mean squared Wasserstein distance with respect to (α, β) : $\min_{\alpha, \beta} n^{-1} \sum_{i=1}^n \mathcal{W}_2^2(F_i, F_i^{\alpha, \beta})$ is equivalent to performing a functional least squares regression based on model (1.2). Note, however, that the resulting least squares estimator does not produce a consistent estimate of (α_0, β_0) because of the endogeneity of \bar{q}_i . To circumvent the endogeneity issue, we introduce a penalized 2SLS method in the next section.

It is also worth noting that the spatially lagged quantile \bar{q}_i corresponds to the quantile function of the spatially weighted *Fréchet mean* \bar{F}_i of $\{F_1, \dots, F_n\}$ at the location of i : $\bar{F}_i := \arg \min_F \sum_{j=1}^n w_{i,j} \mathcal{W}_2^2(F, F_j)$, which is also referred to as the *Wasserstein barycenter*, with $w_{i,j} \geq 0$ and $\sum_{j=1}^n w_{i,j} = 1$. Rather than using \bar{q}_i , one might consider employing the quantile function of the spatially lagged CDF: $\sum_{j=1}^n w_{i,j} F_j$ as the spatial trend term. However, a linear mixture of CDFs is generally multimodal and does not inherit the shape properties of the original CDFs. In this regard, the weighted Fréchet mean should be more representative and faithful as an indicator of the neighborhood trend. This point is also highlighted in [Gunsilius \(2023\)](#) in the context of synthetic control analysis.

²Formally, the Wasserstein distance is a distance between two probability measures. We abuse the notation using CDFs in its arguments for ease of explanation. For more precise discussions on the properties of Wasserstein distance, see [Panaretos and Zemel \(2020\)](#), for instance.

3 Estimation and Asymptotics

3.1 Penalized 2SLS estimator

We now discuss the estimation of α_0 and β_0 . Let $\{\phi_k : k = 1, 2, \dots\}$ be a series of basis functions, such as Fourier series, B-splines, and wavelets, such that we can expand $\alpha_0(t, s) = \sum_{k=1}^{\infty} \phi_k(t)\theta_{0k}(s)$ for each s . Then, we have $\int_0^1 q_i(t)\alpha_0(t, s)dt = \sum_{k=1}^{\infty} r_{i,k}\theta_{0k}(s)$, where $r_{i,k} := \int_0^1 q_i(t)\phi_k(t)dt$. Hence, our model (1.2) can be re-written as

$$q_i(s) = \sum_{k=1}^K \bar{r}_{i,k}\theta_{0k}(s) + x_i^\top \beta_0(s) + \varepsilon_i(s) + u_i(s)$$

where $\bar{r}_{i,k} := \sum_{j=1}^n w_{i,j}r_{j,k}$, $u_i(s) := \int_0^1 \bar{q}_i(t)\alpha_0(t, s)dt - \sum_{k=1}^K \bar{r}_{i,k}\theta_{0k}(s)$, and $K \equiv K_n$ is a sequence of integers tending to infinity as n grows. Note that this is just a multiple regression model having K endogenous regressors $\bar{r}_i = (\bar{r}_{i,1}, \dots, \bar{r}_{i,K})^\top$ with a composite error term $\varepsilon_i(s) + u_i(s)$. Thus, we can resort to the 2SLS approach to estimate $\theta_0(s) = (\theta_{01}(s), \dots, \theta_{0K}(s))^\top$ and $\beta_0(s)$ under the availability of a sufficient number of valid IVs for \bar{r}_i .

Suppose that we have an $L \times 1$ vector $z_{1,i}$ of IVs that are correlated with \bar{r}_i but not with ε_i such that $L \equiv L_n \geq K_n$. The choice of IVs will be discussed later. Further, let $z_i = (z_{1,i}^\top, x_i^\top)^\top$, $Z = (z_1, \dots, z_n)^\top$, $\bar{R} = (\bar{r}_1, \dots, \bar{r}_n)^\top$, $M_z = Z(Z^\top Z)^{-1}Z^\top$, $M_x = X(X^\top X)^{-1}X^\top$, and $\bar{R}_x = (I_n - M_x)\bar{R}$. Then, our 2SLS estimator is defined as follows:

$$\begin{aligned} \hat{\beta}_n(s) &:= [X^\top (I_n - S)X]^{-1} X^\top (I_n - S)Q(s) \\ \hat{\theta}_n(s) &:= [\bar{R}_x^\top M_z \bar{R}_x + \lambda Dn]^{-1} \bar{R}_x^\top M_z Q(s) \end{aligned} \tag{3.1}$$

for a given evaluation point $s \in (0, 1)$, where $S = M_z \bar{R} [\bar{R}^\top M_z \bar{R}]^{-1} \bar{R}^\top M_z$, $\lambda \equiv \lambda_n$ is a non-negative regularization parameter tending to zero as n increases, and D denotes a K -dimensional matrix, which is positive semidefinite, symmetric, and satisfies $\rho_{\max}(D) \lesssim 1$ uniformly in K . Once $\hat{\theta}_n(s) = (\hat{\theta}_{n1}(s), \dots, \hat{\theta}_{nK}(s))^\top$ is obtained, we can estimate $\alpha_0(\cdot, s)$ by

$$\hat{\alpha}_n(\cdot, s) := \sum_{k=1}^K \phi_k(\cdot) \hat{\theta}_{nk}(s).$$

To recover the entire functional form of $\alpha_0(\cdot, \cdot)$ and $\beta_0(\cdot)$, we can repeat the described estimation procedure over a sufficiently fine grid on $[0, 1]$.

Remark 3.1 (Choice of instruments). Observing that $\bar{q}_i(s) \approx \int_0^1 \bar{q}_i(t)\alpha_0(t, s)dt + \bar{x}_i^\top \beta_0(s)$, where $\bar{q}_i(t) := \sum_{j=1}^n w_{i,j}\bar{q}_j(t)$, and $\bar{x}_i := \sum_{j=1}^n w_{i,j}x_j$, the spatially lagged covariates \bar{x}_i would be natural IV candidates for $\bar{r}_{i,k} = \int_0^1 \bar{q}_i(t)\phi_k(t)dt$, assuming that $\beta_0 \neq 0$. For identification, the number of valid IVs must be larger than or equal to K . While it is theoretically required that K tends to infinity as n increases to consistently estimate $\alpha_0(\cdot, s)$, the dimension of \bar{x}_i , d_x , is fixed in our model. Note that, as long as both α_0 and β_0 are non-degenerate, it is possible to create arbitrarily many IVs by taking the spatial lags of x_i of higher and higher order: \bar{x}_i , $\bar{\bar{x}}_i$, ... and so forth. However, the higher the order, the weaker the

instruments. Since K is at most less than eight or so for most practical sample sizes, we believe that finding sufficient IVs may not be a serious concern in most empirical situations where researchers can collect a reasonable number of independent variables. See Remark 3.2 below for a related discussion.

In practice, the 2SLS estimator in (3.1) would be rarely feasible because function q_i can usually only be incompletely observed. For instance, we might only be able to observe the values of q_i at finite points, $q_i(s_{i,1}), \dots, q_i(s_{i,m_i})$. This is the case of our empirical analysis of the age distribution in Japanese cities. In this empirical analysis, we cannot access the complete age distribution for each city, but we only know the distribution up to every five-year age interval. In such a case, for example, we can apply a linear interpolation method to obtain an approximation of the entire functional form of q_i . Without loss of generality, suppose the observations are ordered in an increasing way: $s_{i,1} \leq s_{i,2} \leq \dots \leq s_{i,m_i}$. Then, for each given $s \in [s_{i,l}, s_{i,l+1}]$, we estimate $q_i(s)$ by

$$\hat{q}_i(s) = \omega_i(s)q_i(s_{i,l}) + (1 - \omega_i(s))q_i(s_{i,l+1}), \quad (3.2)$$

where $\omega_i(s) = (s_{i,l+1} - s)/(s_{i,l+1} - s_{i,l})$. When $s < s_{i,1}$ (resp. $s > s_{i,m_i}$), we can set $\hat{q}_i(s) = q(s_{i,1})$ (resp. $\hat{q}_i(s) = q(s_{i,m_i})$).

When q_i is a quantile function, it is also typical that a finite sample $\{y_{i,1}, \dots, y_{i,m_i}\}$ randomly drawn from F_i is only available. In this case, a straightforward approach to estimate q_i would be to perform a nonparametric kernel CDF estimation and invert the estimate. Alternatively, we can also use a simple interpolation method as described in Yang (2020).

Letting \hat{q}_i be any estimator of q_i , compute $\hat{r}_{i,k} := \sum_{j=1}^n w_{i,j} \int_0^1 \hat{q}_j(t) \phi_k(t) dt$ and let $\hat{r}_i = (\hat{r}_{i,1}, \dots, \hat{r}_{i,K})^\top$. Now, the feasible version of (3.1) is defined as

$$\begin{aligned} \tilde{\beta}_n(s) &:= \left[X^\top (I_n - \hat{S}) X \right]^{-1} X^\top (I_n - \hat{S}) \hat{Q}(s) \\ \tilde{\theta}_n(s) &:= \left[\hat{R}_x^\top M_z \hat{R}_x + \lambda Dn \right]^{-1} \hat{R}_x^\top M_z \hat{Q}(s) \end{aligned}$$

where $\hat{Q}(s) = (\hat{q}_1(s), \dots, \hat{q}_n(s))^\top$, $\hat{R} = (\hat{r}_1, \dots, \hat{r}_n)^\top$, $\hat{R}_x = (I_n - M_x) \hat{R}$, and $\hat{S} = M_z \hat{R} [\hat{R}^\top M_z \hat{R}]^{-1} \hat{R}^\top M_z$. The estimator for $\alpha_0(\cdot, s)$ can be obtained by $\tilde{\alpha}_n(\cdot, s) := \sum_{k=1}^K \phi_k(\cdot) \tilde{\theta}_{nk}(s)$.

3.2 Convergence rates and limiting distributions

To derive the asymptotic properties of our estimators, we first need to specify the structure of our sampling space. Following Jenish and Prucha (2012), let $\mathcal{D} \subset \mathbb{R}^d$, $1 \leq d < \infty$ be a possibly uneven lattice, and $\mathcal{D}_n \subset \mathcal{D}$ be the set of observation locations, which may differ across different n . For spatial data, \mathcal{D} would be defined by a geographical space with $d = 2$. Notably, \mathcal{D} does not necessarily have to be exactly observable to us. For example, \mathcal{D} is possibly a complex space of general social and economic characteristics. In this case, we can consider it to be an embedding of individuals in a latent space, instead of their physical locations.

Assumption 3.1. (i) The maximum coordinate difference between any two observations $i, j \in \mathcal{D}$, which we denote as $\Delta(i, j)$, is at least (without loss of generality) 1; and (ii) a threshold distance $\bar{\Delta}$ exists such that $w_{i,j} = 0$ if $\Delta(i, j) > \bar{\Delta}$.

Assumptions 3.1(i) and (ii) together imply that the number of interacting neighbors for each unit is bounded. We believe this is not too restrictive in practice.

Assumption 3.2. (i) $\{z_i\}_{i=1}^n$ are non-stochastic and uniformly bounded; and (ii) $\lim_{n \rightarrow \infty} Z^\top Z/n$ exists and is nonsingular.

Assumption 3.3. (i) For all i , $\varepsilon_i \in L^p(0, 1)$ for some $2 \leq p < \infty$; (ii) $\{\varepsilon_i\}_{i=1}^n$ are independent; and (iii) $\mathbb{E}[\varepsilon_i(s)] = 0$ for all i , $\inf_{1 \leq i \leq n; n \geq 1} \|\varepsilon_i(s)\|_2 > 0$, and $\sup_{1 \leq i \leq n; n \geq 1} \|\varepsilon_i(s)\|_4 \lesssim 1$.

Assumption 3.2(i) states that the covariates and instruments are constant. The same type of assumption as this has been often utilized in the literatures on spatial econometrics and many-IV estimation (e.g., Kelejian and Prucha, 2010; Hausman *et al.*, 2012). Note that this assumption is essentially equivalent to considering all stochastic arguments as being conditional on $\{z_i\}_{i=1}^n$. Assumption 3.3 restricts the distribution of the error functions, which accommodates virtually any form of heteroscedasticity. We might be able to relax the independence assumption in (ii) to some weak dependence condition, but we introduce this for technical simplicity. The s in (iii) is a given interior point of $[0, 1]$ at which the estimation is performed.

Assumption 3.4. (i) For all k , $\phi_k \in L^2(0, 1)$; (ii) $\|\alpha_0(\cdot, s) - \phi_K(\cdot)^\top \theta_0(s)\|_{L^2} \leq \ell_K(s)$, where $\phi_K = (\phi_1, \dots, \phi_K)^\top$; and (iii) $\rho_{\max}(\int_0^1 \phi_K(t) \phi_K(t)^\top dt) \lesssim 1$.

Assumption 3.4 imposes a set of conditions on the basis functions. The L^2 -convergence rate of the approximation errors for various bases is discussed in Belloni *et al.* (2015), where it is shown that $\ell_K(s) \lesssim K^{-\pi}$ typically holds when $\alpha_0(\cdot, s)$ is a π -smooth function (i.e., Hölder class of smoothness order π).

Assumption 3.5. (i) $\rho_{\max}(\mathbb{E}[\bar{R}^\top Z/n] \mathbb{E}[Z^\top \bar{R}/n])$, $\rho_{\max}(\mathbb{E}[\bar{R}_x^\top Z/n] \mathbb{E}[Z^\top \bar{R}_x/n]) \lesssim 1$; and (ii) there exists $\nu_{KL} > 0$ such that $\nu_{KL} \leq \liminf_{n \rightarrow \infty} \rho_{\min}(\mathbb{E}[\bar{R}^\top Z/n] \mathbb{E}[Z^\top \bar{R}/n])$, $\liminf_{n \rightarrow \infty} \rho_{\min}(\mathbb{E}[\bar{R}_x^\top Z/n] \mathbb{E}[Z^\top \bar{R}_x/n])$.

Remark 3.2 (Potentially weak identification of α_0). The ν_{KL} in Assumption 3.5(ii) governs the strength of the identification of α_0 , conceptually equivalent to the issue of *ill-posedness estimation* in high-dimensional IV regression models (Breunig *et al.*, 2020). It is important to note that, the ill-posedness problem in our context is a more practical concern, unlike the intrinsically ill-posed nature of nonparametric IV models (e.g., Blundell *et al.*, 2007; Hoshino, 2022). As mentioned in Remark 3.1, our model assumes only a finite number of exogenous variables (i.e., x_i), while the number of endogenous variables grows to infinity. One potential strategy for constructing a sufficient number of IVs is to use higher-order spatial lags of x_i . However, as the order of spatial lags increases, their correlation with the endogenous variables inevitably gets weaker, and the IVs themselves typically become more collinear. This results in the ill-posedness problem, slowing down the rate of convergence, and inflating the variance of our estimator. A similar discussion can be found in Tchuente (2019). We introduce the penalty term λD to control the variance inflation by restricting the flexibility of the estimated function.

To state the next assumption, we define the following matrices: $\mathbf{V}_n(s) := \text{diag}\{\mathbb{E}[\varepsilon_1^2(s)], \dots, \mathbb{E}[\varepsilon_n^2(s)]\}$,

$$\Omega_{n,x}(s) := \Psi_{n,x}^\top \mathbf{V}_n(s) \Psi_{n,x}/n,$$

$$\Psi_{n,x} := X - Z(Z^\top Z/n)^{-1} \mathbb{E}(Z^\top \bar{R}/n) \left[\mathbb{E} \bar{R}^\top M_z \mathbb{E} \bar{R}/n \right]^{-1} \mathbb{E}(\bar{R}^\top X/n),$$

$$\Sigma_{n,x} := X^\top X/n - \mathbb{E}(X^\top \bar{R}/n) \left[\mathbb{E} \bar{R}^\top M_z \mathbb{E} \bar{R}/n \right]^{-1} \mathbb{E}(\bar{R}^\top X/n).$$

Assumption 3.6. $\Sigma_x := \lim_{n \rightarrow \infty} \Sigma_{n,x}$ and $\Omega_x(s) := \lim_{n \rightarrow \infty} \Omega_{n,x}(s)$ exist and are nonsingular.

The next theorem gives the convergence rate of our estimator.

Theorem 3.1. Suppose Assumptions 2.1 and 3.1 – 3.6 hold. In addition, assume $L\sqrt{K}/(\nu_{KL}^2\sqrt{n}) \lesssim 1$. Then, we have

$$(i) \quad \|\hat{\beta}_n(s) - \beta_0(s)\| \lesssim_p n^{-1/2}, \quad \text{and} \quad (ii) \quad \|\hat{\alpha}_n(\cdot, s) - \alpha_0(\cdot, s)\|_{L^2} \lesssim_p \frac{\sqrt{K}/\sqrt{n} + \ell_K(s)}{\sqrt{\nu_{KL} + \lambda\rho_D}} + \frac{\lambda\|\theta_0(s)\|_D}{\nu_{KL} + \lambda\rho_D},$$

where $\rho_D := \rho_{\min}(D)$, and $\|\theta_0(s)\|_D := \sqrt{\theta_0(s)^\top D \theta_0(s)}$.

The proofs of Theorem 3.1 and those presented below are somewhat similar in several parts to those in Hoshino (2022), but for completeness, they are all presented in Appendix A. Theorem 3.1(i) shows that the coefficients of x_i can be estimated at the root-n rate. Meanwhile, result (ii) indicates that the L^2 -convergence rate of $\hat{\alpha}_n(\cdot, s)$ is not standard owing to the potential weak identification and the presence of the penalty term λD . We can observe a trade-off that the first term converges to zero quickly by selecting a large λ , while the second term can vanish if we select λ diminishing at a sufficiently fast rate such that $\nu_{KL}/\lambda \rightarrow \infty$. It is clear that the order of $\|\theta_0(s)\|_D$ is bounded by \sqrt{K} . When $\theta_0(s)$ is a sparse vector or it is decaying in the order of basis expansion, $\|\theta_0(s)\|_D \lesssim 1$ might be possible.

Next, define $\sigma_{n,\lambda}(t, s) := \sqrt{\phi_K(t)^\top \Sigma_{n,r,\lambda}^{-1} \Omega_{n,r}(s) \Sigma_{n,r,\lambda}^{-1} \phi_K(t)}$, $\Sigma_{n,r,\lambda} := \mathbb{E} \bar{R}_x^\top M_z \mathbb{E} \bar{R}_x/n + \lambda D$, and $\Omega_{n,r}(s) := \mathbb{E} \bar{R}_x^\top M_z \mathbf{V}_n(s) M_z \mathbb{E} \bar{R}_x/n$. Moreover, let

$$\begin{aligned} \hat{\mathbf{C}}_n(s) &:= [X^\top (I_n - S)X/n]^{-1} \left(X^\top (I_n - S) \hat{\mathbf{V}}_n(s) (I_n - S)X/n \right) [X^\top (I_n - S)X/n]^{-1} \\ [\hat{\sigma}_{n,\lambda}(t, s)]^2 &:= \phi_K(t)^\top \left[\bar{R}_x^\top M_z \bar{R}_x/n + \lambda D \right]^{-1} \left(\bar{R}_x^\top M_z \hat{\mathbf{V}}_n(s) M_z \bar{R}_x/n \right) \left[\bar{R}_x^\top M_z \bar{R}_x/n + \lambda D \right]^{-1} \phi_K(t) \end{aligned}$$

where $\hat{\mathbf{V}}_n(s) := \text{diag}\{\hat{\varepsilon}_1^2(s), \dots, \hat{\varepsilon}_n^2(s)\}$, and $\hat{\varepsilon}_i(s) := q_i(s) - \bar{r}_i^\top \check{\theta}_n(s) - x_i^\top \hat{\beta}_n(s)$, where $\check{\theta}_n(s)$ denotes the estimator of $\theta_0(s)$ obtained following (3.1) with λ set to zero. Then, the limiting distribution of our estimator can be characterized as in the following theorem.

Theorem 3.2. Suppose Assumptions 2.1 and 3.1 – 3.6 hold. In addition, assume

$$\begin{aligned} K \sim L, \quad K^3/(\nu_{KL}^4 n) \rightarrow 0, \quad \sqrt{n} \ell_K(s)/\sqrt{\nu_{KL}} \rightarrow 0, \\ \sqrt{n} |\phi_K(t)^\top \theta_0(s) - \alpha_0(t, s)| / \|\phi_K(t)\| \rightarrow 0, \quad \lambda/\nu_{KL}^2 \rightarrow 0, \quad \sqrt{n} \lambda \|\theta_0(s)\|_D / \nu_{KL} \rightarrow 0. \end{aligned}$$

Then, we have

$$(i) \sqrt{n}(\hat{\beta}_n(s) - \beta_0(s)) \xrightarrow{d} \mathcal{N}(0, \Sigma_x^{-1} \Omega_x(s) \Sigma_x^{-1}), \quad (ii) \frac{\sqrt{n}(\hat{\alpha}_n(t, s) - \alpha_0(t, s))}{\sigma_{n, \lambda}(t, s)} \xrightarrow{d} \mathcal{N}(0, 1),$$

$$(iii) \left\| \hat{\mathbf{C}}_n(s) - \Sigma_x^{-1} \Omega_x(s) \Sigma_x^{-1} \right\| = o_P(1), \text{ and } (iv) |\hat{\sigma}_{n, \lambda}(t, s) - \sigma_{n, \lambda}(t, s)| = o_P(1).$$

Remark 3.3 (Choice of tuning parameters). To implement our estimator, we need to select three tuning parameters λ , K , and L . For the penalty parameter λ , considering the assumptions in Theorem 3.2, it must converge to zero faster at least than $n^{-1/2}$. In the numerical studies presented below, we set $\lambda \sim n^{-3/5}$. For the order of basis expansion K , assume that $L \sim K \sim n^{\bar{k}}$ for some $\bar{k} > 0$. We further assume that the ill-posedness is mild such that $\nu_{KL} \lesssim K^{-\nu}$ for some $\nu > 0$ and suppose that $\alpha_0(\cdot, s)$ is a π -smooth function such that $\ell_K(s) \lesssim K^{-\pi}$. Then, easy calculations yield that K must satisfy $1/(2\pi - \nu) < \bar{k} < 1/(3 + 4\nu)$ to ensure the asymptotic normality results. This clearly indicates that when the IVs are not strong, a modest K should be employed. In Section 4, we numerically examine the impact of tuning parameters selection. The results demonstrate that the choice of λ is more influential on the estimation performance than that of K . More sophisticated, data-driven tuning parameter choice methods will be investigated in future studies.

3.3 Testing the presence of spatial effects

In this section, we consider statistically testing the presence of spatial effects. Specifically, for each given s , we test the following null hypothesis:

$$\mathbb{H}_0 : \alpha_0(t, s) = 0 \text{ almost everywhere } t \in \mathcal{I}$$

where \mathcal{I} denotes a non-degenerate sub-interval of $[0, 1]$. Then, a natural test statistic for testing \mathbb{H}_0 would be the Wald-type statistic given as follows:

$$T_n := n \int_{\mathcal{I}} \hat{\alpha}_n^2(t, s) dt,$$

where the dependence of T_n on s is suppressed. To derive the asymptotic distribution of T_n under \mathbb{H}_0 , let $\Xi_n := \Sigma_{n, r, \lambda}^{-1} \mathbb{E}(\bar{R}_x^\top Z/n) (Z^\top Z/n)^{-}$ and $\Phi_{\mathcal{I}} := \int_{\mathcal{I}} \phi_K(t) \phi_K(t)^\top dt$. Further, define

$$\begin{aligned} \mu_n &:= \text{tr} \left\{ \Xi_n^\top \Phi_{\mathcal{I}} \Xi_n (Z^\top \mathbf{V}_n(s) Z/n) \right\} \\ v_n &:= 2 \text{tr} \left\{ \Xi_n^\top \Phi_{\mathcal{I}} \Xi_n (Z^\top \mathbf{V}_n(s) Z/n) \Xi_n^\top \Phi_{\mathcal{I}} \Xi_n (Z^\top \mathbf{V}_n(s) Z/n) \right\}, \end{aligned}$$

which serve as the mean and variance of T_n , respectively.

Here, we introduce the following miscellaneous assumptions.

Assumption 3.7. (i) $\sup_{1 \leq i \leq n; n \geq 1} \|\varepsilon_i(s)\|_6 \lesssim 1$; and (ii) $0 < \rho_{\min}(\Phi_{\mathcal{I}}) \leq \rho_{\max}(\Phi_{\mathcal{I}}) \lesssim 1$.

The next theorem characterizes the asymptotic distribution of our test statistic.

Theorem 3.3. Suppose Assumption 3.7 and the assumptions in Theorem 3.2 are all satisfied. In addition, assume $1/(K\nu_{KL}^2) \rightarrow 0$ and $K^3/(\nu_{KL}^5 n) \rightarrow 0$. Then, we have $(T_n - \mu_n)/\sqrt{v_n} \xrightarrow{d} \mathcal{N}(0, 1)$.

When \mathbb{H}_0 does not hold, the standardized test statistic $(T_n - \mu_n)/\sqrt{v_n}$ deviates to a positive value. Thus, considering Theorem 3.3, we can reject \mathbb{H}_0 at the $100\alpha\%$ significance level if the realized value of $(T_n - \mu_n)/\sqrt{v_n}$ exceeds the upper α -quantile of $\mathcal{N}(0, 1)$. To implement the test in practice, we need to consistently estimate μ_n and v_n , which can be easily performed by the sample analogue estimators, the definitions of which should be clear from the context. The consistency of these estimators is straightforward (refer to Lemmas A.3 and A.4 and Theorem 3.2(iii), (iv)).

Remark 3.4. The proposed test can easily be extended to a more general null hypothesis: $\mathbb{H}_0 : \alpha_0(t, s) = a(t)$ for $t \in \mathcal{I}$, where $a(\cdot)$ is any given function that is pre-specified by the researcher (or estimable with a certain convergence rate). The resulting test statistic would take the following form: $T_n = \int_{\mathcal{I}} (\hat{\alpha}_n(t, s) - a(t))^2 dt$, and \mathbb{H}_0 can be tested using the same procedure as above.

Finally, it is important to notice that when $\mathbb{H}_0 : \alpha_0(t, s) = 0$ is indeed true over the entire $[0, 1]$, higher-order spatially-lagged covariates are not valid IVs, that is, for example, \bar{x}_i and \bar{q}_i are not related to each other. Thus, basically, we need to prepare a sufficient number of IVs using only \bar{x}_i and possibly its transformations in this case.

3.4 Asymptotic properties under interpolated outcome functions

Finally, in this section, we examine the cases in which the outcome functions are only discretely observed, and they are linearly interpolated following (3.2). Letting $s_{i,0} = 0$ and $s_{i,m_i+1} = 1$ for all i , we introduce the following assumption.

Assumption 3.8. For all i , (i) there exists a positive sequence $\kappa \equiv \kappa_n$ tending to zero as n increases such that $|s_{i,l+1} - s_{i,l}| \lesssim \kappa$, for all $l = 0, 1, \dots, m_i$; and (ii) there exists a constant $\xi \in (0, 1]$ such that $|q_i(s_1) - q_i(s_2)| \lesssim |s_1 - s_2|^\xi$ for any $s_1, s_2 \in [0, 1]$.

Assumption 3.8(i) determines the overall precision of the linear interpolation approximation. For simplicity of discussion, it assumes that the values of the outcome function are (quasi) uniformly observed such that the distance of any two consecutive observations is of order κ . In addition, note that we treat each observation point as nonstochastic. Assumption 3.8(ii) requires that the outcome function is Hölder continuous with exponent ξ for all i . This assumption may be somewhat restrictive, but similar assumptions are often considered in the FDA literature (e.g., Crambes *et al.*, 2009). Obviously, we need some form of continuity in order for the interpolation approximation to work.

The following theorem states that the approximation errors caused by the linear interpolation are asymptotically negligible if κ^ξ is sufficiently small.

Theorem 3.4. Suppose Assumption 3.8 and those in Theorem 3.2 are all satisfied. In addition, assume $\sqrt{n}\kappa^\xi/\sqrt{\nu_{KL}} \rightarrow 0$. Then, $\tilde{\beta}_n(s)$ and $\tilde{\alpha}_n(\cdot, s)$ are asymptotically equivalent to $\hat{\beta}_n(s)$ and $\hat{\alpha}_n(\cdot, s)$, respectively.

Under Assumption 3.8, the approximation error $|\hat{q}_i(s) - q_i(s)|$ is of order κ^ξ uniformly in s . The condition $\sqrt{n}\kappa^\xi/\sqrt{\nu_{KL}} \rightarrow 0$ states that the interpolation error should shrink to zero faster than $n^{-1/2}$, similar to the basis approximation error $\ell_K(s)$. From this result, it is also straightforward to observe the asymptotic equivalence between the feasible Wald test $\tilde{T}_n := n \int_{\mathcal{I}} \tilde{\alpha}_n^2(t, s) dt$ and T_n presented in the previous section.

4 Numerical Experiments

Performance of the 2SLS estimator In this section, we first examine the finite sample performance of the proposed 2SLS estimator. We consider the following three data-generating processes (DGPs) for the Monte Carlo experiments:

$$q_i(s) = \int_0^1 \bar{q}_i(t) \alpha_0(t, s) dt + \sum_{j=1}^7 x_{i,j} \beta_{0j}(s) + \varepsilon_i(s),$$

where

$$\text{DGP 1: } \alpha_0(t, s) = (t + s)/2$$

$$\text{DGP 2: } \alpha_0(t, s) = \text{PDF of } \mathcal{N}(t - s, 0.7^2)$$

$$\text{DGP 3: } \alpha_0(t, s) = 0.3 + 0.7t \sin(2\pi(t - s))$$

$\beta_{0j}(s) = 1 + 1.2 \log(s + 1)$ for $j = 1, 2, 3$, $\beta_{0j}(s) = \exp(s) - 0.4$ for $j = 4, \dots, 7$, $x_{i,j} \stackrel{IID}{\sim} \mathcal{N}(0, 1)$ for all j , and $\varepsilon_i(s) = \varepsilon_{1,i} + \sum_{j=1}^4 s^{j/2} \varepsilon_{2,i,j}$ with $\varepsilon_{1,i} \stackrel{IID}{\sim} \mathcal{N}(0, 0.3^2)$ and $\varepsilon_{2,i,j} \stackrel{IID}{\sim} \mathcal{N}(0, 0.6^2)$ for all j . When estimating the model, an intercept term is also included. We randomly allocate n units on the lattice of $n/20 \times 40$, where we consider two sample sizes: $n \in \{400, 1600\}$. The spatial weight matrix W_n is defined according to the Rook contiguity with row normalization. Since these three DGPs satisfy the requirements in Assumption 2.1, we can generate the outcome functions Q using the Neumann series approximation: $Q \approx Q^{(L)} := \sum_{\ell=0}^L \mathcal{T}^\ell [X\beta_0 + \mathcal{E}]$, where L is increased until $\max_{1 \leq i \leq n} |q_i^{(L)}(s) - q_i^{(L-1)}(s)| < 0.001$ is met for all s . For computing the integrals over $[0, 1]$, we approximate them by finite summations over 199 grid points: 0.005, 0.010, \dots , 0.995.

For the choice of the basis functions $\{\phi_k\}$, we use the cubic B-splines. We examine two values for the number of the inner knots of the B-splines: $\# \text{ knots} \in \{2, 3\}$, corresponding to $K = 6$ and 7, respectively, both of which are equally spaced in $[0, 1]$. The IVs used are the first- and second-order spatial lags of $\{1, x_{i,1}, \dots, x_{i,7}\}$. Note that because there may exist some units that have no neighboring units, the spatial lags of 1 are not necessarily constants. For the penalty term λD , we set $D = I_K$ (i.e., the ridge penalty) and attempt using four values for $\lambda = \lambda_c n^{-3/5}$ with $\lambda_c \in \{0.5, 1, 2, 3\}$. The number of Monte Carlo repetitions for each setup is set to 1000. Throughout, the evaluation point s is fixed at $s = 0.5$.

The performance of the coefficient estimator $\hat{\beta}_n$ is evaluated using the average bias (BIAS) and the average root mean squared error (RMSE):

$$\text{BIAS: } \frac{1}{7} \sum_{j=1}^7 \left[\frac{1}{1000} \sum_{r=1}^{1000} \hat{\beta}_{nj}^{(r)}(s) - \beta_{0j}(s) \right], \quad \text{RMSE: } \frac{1}{7} \sum_{j=1}^7 \left[\frac{1}{1000} \sum_{r=1}^{1000} (\hat{\beta}_{nj}^{(r)}(s) - \beta_{0j}(s))^2 \right]^{1/2},$$

where superscript (r) means that the estimate is obtained from the r -th replicated dataset. Similarly, for the estimator $\hat{\alpha}_n$ of the spatial effect, we evaluate the performance based on the BIAS and RMSE

averaged over the 19 evaluation points $\{t_1, t_2, \dots, t_{19}\}$ equally spaced on $[0, 1]$:

$$\text{BIAS: } \frac{1}{19} \sum_{j=1}^{19} \left[\frac{1}{1000} \sum_{r=1}^{1000} \hat{\alpha}_n^{(r)}(t_j, s) - \alpha_0(t_j, s) \right], \quad \text{RMSE: } \frac{1}{19} \sum_{j=1}^{19} \left[\frac{1}{1000} \sum_{r=1}^{1000} (\hat{\alpha}_n^{(r)}(t_j, s) - \alpha_0(t_j, s))^2 \right]^{1/2}.$$

Table 1 summarizes the simulation results. Our main findings are as follows: First, the results suggest that our estimator works satisfactorily well for all scenarios. The RMSE values for estimating β_0 are approximately halved when the sample size is increased from 400 to 1600, which is consistent with our theorem. Meanwhile, the RMSE values for estimating α_0 do not decrease significantly even when the sample size is increased. This result would be owing to the increased variances caused by employing a smaller penalty parameter λ (recall that $\lambda \sim n^{-3/5}$). When comparing the results of the estimators with different λ values, our results suggest that when the functional form of the spatial effect α_0 is simple as in DGPs 1 and 2, using an estimator with a relatively large penalty is advisable in terms of RMSE. In contrast, when the functional form of α_0 is complex as in DGP 3, the estimator with the smallest penalty outperforms the others, which should be a reasonable result. It seems that the number of inner knots has only minute impacts on the estimation performance.

Table 1: Estimation performance

DGP	n	# knots	β		$\alpha (\lambda_c = 0.5)$		$\alpha (\lambda_c = 1)$		$\alpha (\lambda_c = 2)$		$\alpha (\lambda_c = 3)$	
			BIAS	RMSE	BIAS	RMSE	BIAS	RMSE	BIAS	RMSE	BIAS	RMSE
1	400	2	-0.0010	0.0361	0.0201	0.1059	0.0213	0.1024	0.0188	0.1009	0.0147	0.0996
		3	-0.0010	0.0362	0.0207	0.1186	0.0216	0.1146	0.0183	0.1124	0.0135	0.1108
	1600	2	-0.0004	0.0178	0.0151	0.0957	0.0189	0.0950	0.0209	0.0967	0.0207	0.0979
		3	-0.0004	0.0178	0.0160	0.1100	0.0196	0.1085	0.0213	0.1093	0.0207	0.1101
2	400	2	-0.0017	0.0365	-0.0010	0.0922	-0.0054	0.0836	-0.0124	0.0776	-0.0187	0.0748
		3	-0.0018	0.0366	-0.0010	0.1079	-0.0057	0.0997	-0.0133	0.0937	-0.0202	0.0908
	1600	2	-0.0006	0.0179	0.0014	0.0852	-0.0011	0.0814	-0.0048	0.0781	-0.0080	0.0764
		3	-0.0006	0.0179	0.0015	0.1018	-0.0010	0.0981	-0.0050	0.0948	-0.0084	0.0931
3	400	2	-0.0017	0.0394	0.0148	0.1821	0.0177	0.1944	0.0155	0.2060	0.0107	0.2111
		3	-0.0017	0.0394	0.0154	0.1850	0.0177	0.1991	0.0144	0.2115	0.0088	0.2165
	1600	2	-0.0006	0.0192	0.0077	0.1544	0.0133	0.1680	0.0172	0.1860	0.0175	0.1955
		3	-0.0006	0.0192	0.0087	0.1531	0.0140	0.1705	0.0173	0.1906	0.0172	0.2008

Performance of the Wald test Next, we assess the finite sample performance of our test for the presence of spatial effects. In this analysis, we use the same DGP as given above to generate the data, with a slight modification on α_0 in DGP 2. Specifically,

$$\alpha_0(t, s) = \varrho \times \text{PDF of } \mathcal{N}(t - s, 0.7^2),$$

where $\varrho \in \{0, 0.1, 0.2\}$. The null hypothesis to be tested is $\mathbb{H}_0 : \alpha_0(t, 0.5) = 0$ for $t \in [0.1, 0.9]$. Thus, \mathbb{H}_0 holds true when $\varrho = 0$.

In Table 2, we present the rejection frequency over 1000 Monte Carlo repetitions at the 10%, 5%, and 1% significance levels. The results for $\varrho = 0$ demonstrate that the size of our test is reasonably

well-controlled, with at most 1–2% deviation from the nominal levels for most cases. When the spatial effect is mild in magnitude ($\varrho = 0.1$), the estimator with a smaller penalty ($\lambda_c = 0.5$) is not sufficiently powerful to detect the effect probably owing to its large estimation variance. However, as expected, the power of the test can be significantly improved by increasing the sample size. In the case of a stronger spatial effect ($\varrho = 0.2$), all tests exhibit nearly perfect power property for all sample sizes.

Table 2: Rejection frequency

# knots	n	λ_c	$\varrho = 0$			$\varrho = 0.1$			$\varrho = 0.2$			
			10%	5%	1%	10%	5%	1%	10%	5%	1%	
2	400	0.5	0.085	0.048	0.023	0.315	0.231	0.128	0.985	0.974	0.900	
		1	0.080	0.054	0.021	0.762	0.686	0.497	1.000	1.000	0.998	
		2	0.074	0.047	0.018	0.971	0.956	0.908	1.000	1.000	1.000	
		3	0.068	0.047	0.022	0.982	0.977	0.959	1.000	1.000	1.000	
	1600	0.5	0.081	0.058	0.030	0.642	0.474	0.260	1.000	1.000	1.000	
		1	0.084	0.056	0.029	0.980	0.951	0.811	1.000	1.000	1.000	
		2	0.087	0.057	0.029	1.000	1.000	1.000	1.000	1.000	1.000	
		3	0.086	0.056	0.027	1.000	1.000	1.000	1.000	1.000	1.000	
	3	400	0.5	0.085	0.048	0.023	0.322	0.236	0.129	0.986	0.976	0.912
			1	0.080	0.053	0.021	0.782	0.695	0.516	1.000	1.000	0.998
			2	0.077	0.046	0.017	0.972	0.957	0.915	1.000	1.000	1.000
			3	0.069	0.047	0.023	0.982	0.979	0.962	1.000	1.000	1.000
1600		0.5	0.077	0.054	0.028	0.624	0.457	0.243	1.000	1.000	1.000	
		1	0.081	0.055	0.028	0.979	0.952	0.817	1.000	1.000	1.000	
		2	0.085	0.055	0.028	1.000	1.000	1.000	1.000	1.000	1.000	
		3	0.081	0.053	0.027	1.000	1.000	1.000	1.000	1.000	1.000	

Simulations under discretely observed outcome functions Finally, we evaluate the performance of our estimator and test when the entire shapes of the outcome functions are not perfectly observed but their values are discretely observable at finite points. The DGPs investigated here are identical to those used previously. To recover the entire functional form of the outcome function for each unit, we use the linear interpolation method in (3.2). For all units, we assume that m pairs of points $\{(s_{i,j}, q_i(s_{i,j}))\}_{j=1}^m$ are observable, where $s_{i,j}$'s are uniformly randomly drawn from $[0, 1]$, and m is selected from two values $m \in \{15, 50\}$.

To save space, the simulation results are omitted here and provided in Tables B1 and B2 in Appendix B. From these tables, we can observe similar overall tendencies as those shown above. An interesting finding is that, although increasing m from 15 to 50 improves the RMSE for most cases, there are some situations in which the estimator with a smaller m achieves an even slightly better RMSE. Similarly, comparing the results when $m = 15$ with those when the outcome function is fully observable (those reported in Table 1), the former occasionally exhibits smaller RMSE values. We conjecture that these phenomena occurred because the linear interpolation “smoothed out” the original, potentially noisier, outcome function, leading to a reduction in estimation variance. A similar discussion can be found in [Imaizumi and Kato \(2018\)](#) in a different but related context. In contrast, regarding the size property of the Wald test, the linear interpolation seems to introduce certain distortions. Unsurprisingly, these distortions can be somewhat mitigated if m is large. Except when $\lambda_c = 0.5$, the test exhibits a satisfactory power for both values of m .

5 An Empirical Illustration: Age Distribution of Japanese Cities

In this section, we apply the proposed estimator and test to analyze the determinants of the age distribution of Japanese cities. While this type of data has been regularly studied in the FDA literature (e.g., [Delicado, 2011](#); [Hron *et al.*, 2016](#); [Bigot *et al.*, 2017](#)), there are few papers attempting a regression-based analysis. In recent decades, many rural Japanese cities have been facing a serious aging population, prompting them to plan campaigns to encourage young people from urban areas to settle in their cities. Thus, investigating the relationship between the regional socioeconomic characteristics and the age structure and the impact of neighborhood trend on it would be meaningful.

Our sample comprises all local municipalities (*Shi-ku-cho-son*) in Japan. The age distribution data for each city are taken from the 2020 Census. For the covariates to explain the age distribution, we use the ratio of agricultural, forestry, and fishery workers, number of hospital beds per capita, number of childcare facilities per capita, unemployment rate, logarithm of annual commercial sales, and logarithm of average residential landprice. All variables are as of the most recent year before 2020, and they are all publicly available.³ In addition to these, we include five regional dummies.⁴ After excluding the observations with missing items, the analysis is performed on 1883 municipalities. Table C3 in Appendix C summarizes the detailed definitions of the variables used and their basic statistics.

Our age distribution data are not complete; we only have information on the population size at five-year intervals (0 – 4 years old, 5 – 9 years old, and so forth). Therefore, when computing the quantile function for each city, we performed the linear interpolation as in (3.2). In Figure 1, we depict the obtained quantile functions for 20 randomly selected cities from our dataset. The figure clearly shows the existence of certain regional heterogeneity in age compositions except those close to the boundary points.

For estimation, we follow the same procedure as in the previous section with $K = 7$ (three inner knots) and $\lambda = 3n^{-3/5}$. The integrals are replaced by summations over 399 equally-spaced grid points on $[0, 1]$. For the spatial weight, expecting that the impacts from demographic changes in large cities should be larger than those from small cities, we consider the following specification:

$$w_{i,j} = \frac{\mathbf{1}\{i \text{ and } j \text{ are adjacent}\} \sqrt{\text{Population}_j}}{\sum_{j \neq i} \mathbf{1}\{i \text{ and } j \text{ are adjacent}\} \sqrt{\text{Population}_j}}.$$

When city i has no neighbors (e.g., islands), we set $w_{i,j} = 0$ for all j . The estimation is performed on nine quantile values: $s = 0.1, 0.2, \dots, 0.9$.

To save space, the estimated coefficients $\beta_0(s)$ are presented in Figure C1 in Appendix C. Our major findings from the figure are as follows: Interestingly, for all variables, the impacts on age distribution become prominent around the median ($s = 0.5$), suggesting the residential flexibility of this age group in response to the socioeconomic conditions of a city. The variables considered as indicators of urbanness, such as the commercial sales and the landprice, exhibit negative effects, contributing to population rejuvenation. As expected, cities with a higher rate of agricultural workers exhibit a significant aging

³Landprice data: <https://www.lic.or.jp/landinfo/research.html>; all others: <https://www.e-stat.go.jp/en>.

⁴They correspond to each of the following: *Hokkaido-Tohoku*, *Chubu*, *Kinki*, *Chugoku-Shikoku*, and *Kyushu-Okinawa* regions.

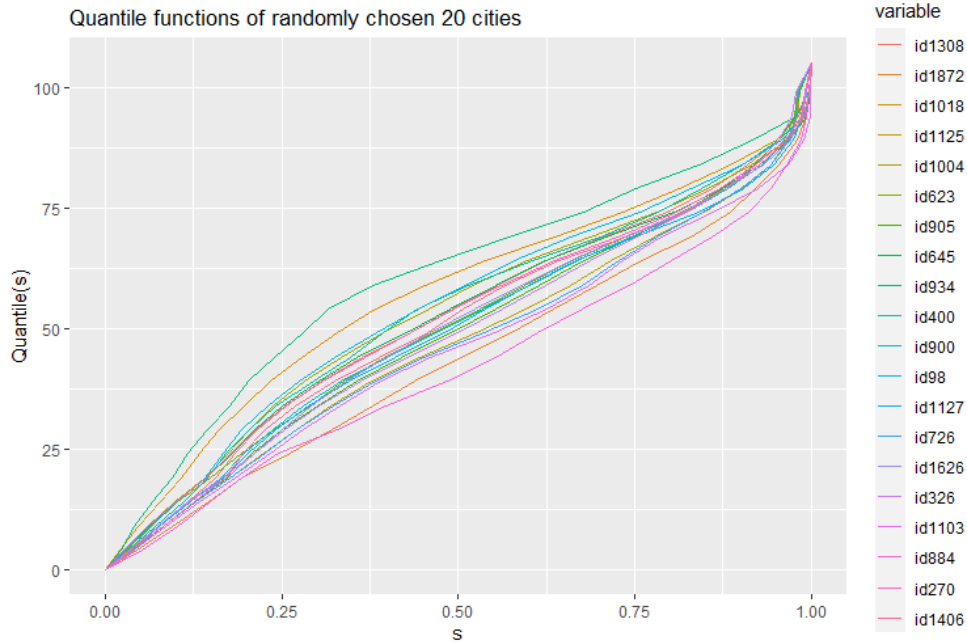


Figure 1: Age quantile functions of randomly selected cities

trend. Both the number of hospital beds and childcare facilities positively affect age distribution, although the underlying mechanisms are unclear. It is important to recall that in this study, the covariates are treated as fixed, and their potential endogeneity is ignored. To interpret the obtained results as a causal relationship, addressing the endogeneity issue more carefully would be necessary.

The estimated spatial effect function is reported in Figure 2. The figure includes nine panels, each corresponding to different s -values. In the figure, we also report the computed test statistic $(T_n - \mu_n)/\sqrt{v_n}$ for $\mathcal{I} = [0, 1]$. From these results, we can observe the following: First, the values of the test statistic suggest that the spatial effects exist significantly at all nine quantiles. However, when quantile t of the neighbor is close to either of the boundary points 0 or 1, almost no or weak spatial effects are present. This seems reasonable considering Figure 1; only a little regional heterogeneity in age distribution is present at these extreme quantiles. The spatial interaction effects become particularly strong when both t and s are approximately 0.2 – 0.5, which roughly correspond to the ages of the younger working population. This result might suggest that the growth of economic activities and their spillovers play main roles in forming the spatial trend of age distribution. Notably, the impacts from these lower-to-middle quantile values somewhat persist even for higher quantile ages. This could be reflecting the indirect effects from positive interactions among younger age groups, rather than a direct causal relationship across different quantiles.

6 Conclusion

In this study, we developed a new SAR model for analyzing spatial interactions among functional outcomes. For estimation, we developed a penalized 2SLS estimator and established its asymptotic properties under certain regularity conditions. Additionally, we developed a method for statistically

testing the presence of spatial interactions. To illustrate the effectiveness of our proposed method, we performed an empirical analysis focusing on the age distribution in Japanese cities.

An important potential limitation of our study is that, while we have treated the covariates as fixed variables to simplify the theoretical exposition, this approach essentially obscures the endogeneity issue underlying the covariates. For instance, in our empirical analysis, it might be reasonable to consider the unemployment rate as an endogenous variable correlated with unobserved regional factors affecting the age distribution as well. One way to mitigate the endogeneity issue would be to extend the current model to a panel data model with functional fixed effects, which should be a promising topic for future studies. Another important future work is how to perform the estimation and inference when α_0 and β_0 are not significant, leading to a weak IV problem. We conjecture that the inclusion of additional moment conditions based on the distribution of the error term might be effective in addressing this issue, as in [Lee \(2007\)](#). Several other issues that need future investigation include: data-driven selection of tuning parameters and developing methods for uniform inference on the functional parameters.

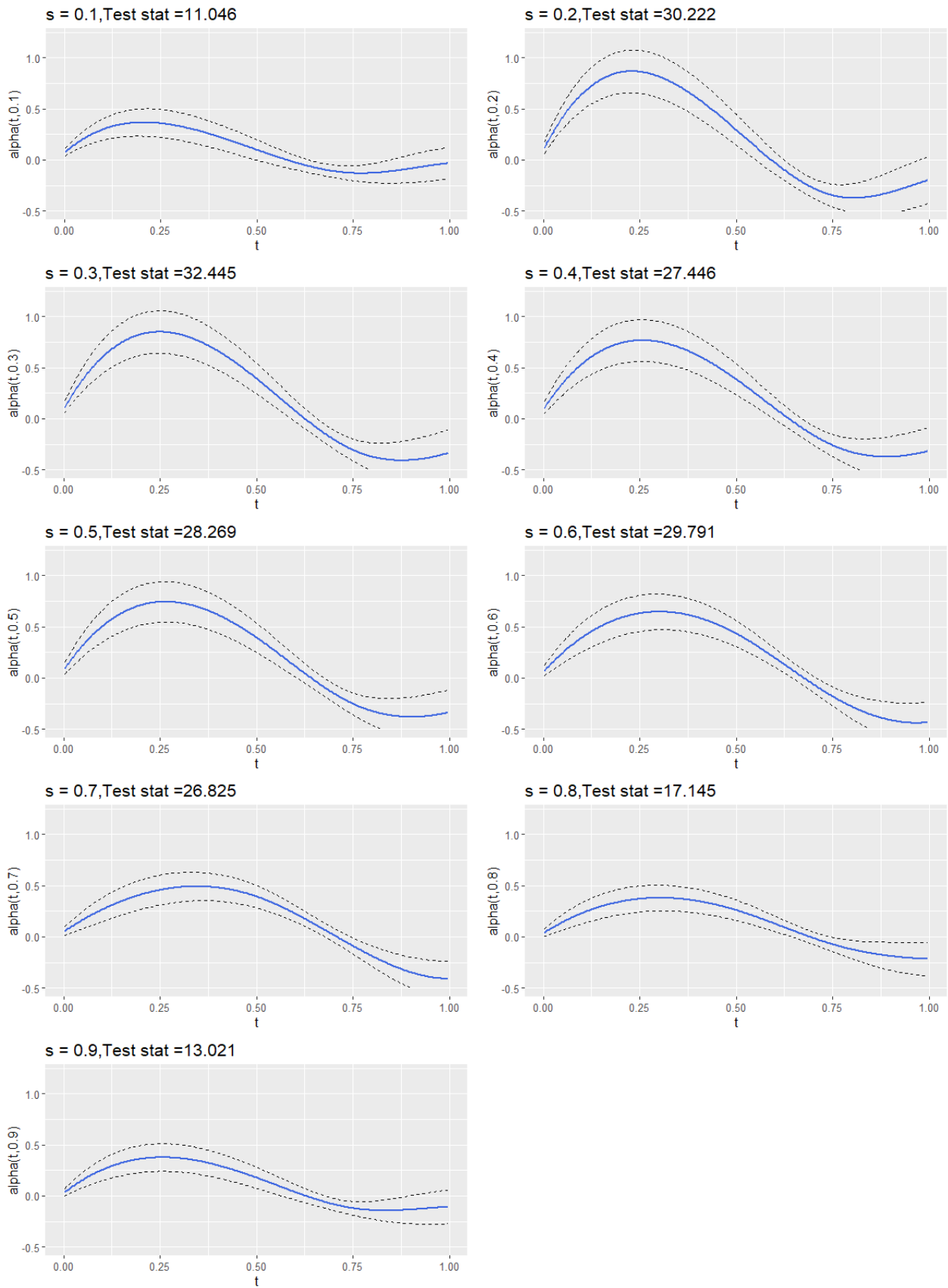


Figure 2: Estimated spatial effect function

In each panel, the solid line indicates the estimated $\alpha_0(\cdot, s)$, and the dotted lines indicate the 95% confidence interval.

References

- Ando, T., Li, K., and Lu, L., 2023. A spatial panel quantile model with unobserved heterogeneity, *Journal of Econometrics*, 232 (1), 191–213.
- Belloni, A., Chernozhukov, V., Chetverikov, D., and Kato, K., 2015. Some new asymptotic theory for least squares series: Pointwise and uniform results, *Journal of Econometrics*, 186 (2), 345–366.
- Bigot, J., Gouet, R., Klein, T., and López, A., 2017. Geodesic pca in the wasserstein space by convex pca, *Annales de l'Institut Henri Poincaré, Probabilités et Statistiques*, 53 (1), 1 – 26.
- Blundell, R., Chen, X., and Kristensen, D., 2007. Semi-nonparametric iv estimation of shape-invariant Engel curves, *Econometrica*, 75 (6), 1613–1669.
- Breunig, C., Mammen, E., and Simoni, A., 2020. Ill-posed estimation in high-dimensional models with instrumental variables, *Journal of Econometrics*, 219 (1), 171–200.
- Chen, Y., Lin, Z., and Müller, H.G., 2023. Wasserstein regression, *Journal of the American Statistical Association*, 118 (542), 869–882.
- Crambes, C., Kneip, A., and Sarda, P., 2009. Smoothing splines estimators for functional linear regression, *The Annals of Statistics*, 37 (1), 35–72.
- de Jong, P., 1987. A central limit theorem for generalized quadratic forms, *Probability Theory and Related Fields*, 75 (2), 261–277.
- Delicado, P., 2011. Dimensionality reduction when data are density functions, *Computational Statistics & Data Analysis*, 55 (1), 401–420.
- Dong, C., Chen, R., Xiao, Z., and Liu, W., 2024. Functional quantile autoregression, *Journal of Econometrics*, forthcoming.
- Dudley, R.M. and Philipp, W., 1983. Invariance principles for sums of Banach space valued random elements and empirical processes, *Zeitschrift für Wahrscheinlichkeitstheorie und verwandte Gebiete*, 62 (4), 509–552.
- Ghodrati, L. and Panaretos, V.M., 2022. Distribution-on-distribution regression via optimal transport maps, *Biometrika*, 109 (4), 957–974.
- Gunsilius, F.F., 2023. Distributional synthetic controls, *Econometrica*, 91 (3), 1105–1117.
- Han, K., Müller, H.G., and Park, B.U., 2020. Additive functional regression for densities as responses, *Journal of the American Statistical Association*, 115 (530), 997–1010.
- Hausman, J.A., Newey, W.K., Woutersen, T., Chao, J.C., and Swanson, N.R., 2012. Instrumental variable estimation with heteroskedasticity and many instruments, *Quantitative Economics*, 3 (2), 211–255.

- Hoshino, T., 2022. Sieve IV estimation of cross-sectional interaction models with nonparametric endogenous effect, *Journal of Econometrics*, 229 (2), 263–275.
- Hron, K., Menafoglio, A., Templ, M., Hruzová, K., and Filzmoser, P., 2016. Simplicial principal component analysis for density functions in bayes spaces, *Computational Statistics & Data Analysis*, 94, 330–350.
- Imaizumi, M. and Kato, K., 2018. PCA-based estimation for functional linear regression with functional responses, *Journal of Multivariate Analysis*, 163, 15–36.
- Jenish, N., 2012. Nonparametric spatial regression under near-epoch dependence, *Journal of Econometrics*, 167 (1), 224–239.
- Jenish, N. and Prucha, I.R., 2009. Central limit theorems and uniform laws of large numbers for arrays of random fields, *Journal of Econometrics*, 150 (1), 86–98.
- Jenish, N. and Prucha, I.R., 2012. On spatial processes and asymptotic inference under near-epoch dependence, *Journal of Econometrics*, 170 (1), 178–190.
- Kelejian, H.H. and Prucha, I.R., 2010. Specification and estimation of spatial autoregressive models with autoregressive and heteroskedastic disturbances, *Journal of Econometrics*, 157 (1), 53–67.
- Kress, R., 2014. *Linear Integral Equations, Third Edition*, Springer.
- Lee, L.f., 2007. GMM and 2SLS estimation of mixed regressive, spatial autoregressive models, *Journal of Econometrics*, 137 (2), 489–514.
- Malikov, E., Sun, Y., and Hite, D., 2019. (Under) mining local residential property values: A semi-parametric spatial quantile autoregression, *Journal of Applied Econometrics*, 34 (1), 82–109.
- Panaretos, V.M. and Zemel, Y., 2020. *An Invitation to Statistics in Wasserstein Space*, Springer.
- Petersen, A., Liu, X., and Divani, A.A., 2021. Wasserstein F-tests and confidence bands for the Fréchet regression of density response curves, *The Annals of Statistics*, 49 (1), 590–611.
- Petersen, A. and Müller, H.G., 2016. Functional data analysis for density functions by transformation to a Hilbert space, *The Annals of Statistics*, 183–218.
- Petersen, A., Zhang, C., and Kokoszka, P., 2022. Modeling probability density functions as data objects, *Econometrics and Statistics*, 21, 159–178.
- Ramsay, J. and Silverman, B., 2005. *Functional Data Analysis*, Springer.
- Su, L. and Yang, Z., 2011. Instrumental variable quantile estimation of spatial autoregressive models, *Working Paper*.
- Tchuente, G., 2019. Weak identification and estimation of social interaction models, *arXiv preprint arXiv:1902.06143*.

- Yang, H., 2020. Random distributional response model based on spline method, *Journal of Statistical Planning and Inference*, 207, 27–44.
- Yang, H., Baladandayuthapani, V., Rao, A.U., and Morris, J.S., 2020. Quantile function on scalar regression analysis for distributional data, *Journal of the American Statistical Association*, 115 (529), 90–106.
- Zhu, X., Cai, Z., and Ma, Y., 2022. Network functional varying coefficient model, *Journal of the American Statistical Association*, 117 (540), 2074–2085.

Appendix

A Proofs

Definition A.1. Let $\mathbf{x} = \{x_{n,i} : i \in \mathcal{D}_n; n \geq 1\}$ and $\mathbf{e} = \{e_{n,i} : i \in \mathcal{D}_n; n \geq 1\}$ be triangular arrays of random fields, where x and e are real-valued and general (possibly infinite-dimensional) random variables, respectively. Then, the random field \mathbf{x} is said to be L^p -near-epoch dependent (NED) on \mathbf{e} if

$$\|x_{n,i} - \mathbb{E}[x_{n,i} \mid \mathcal{F}_{n,i}(\delta)]\|_p \leq c_{n,i}\varphi(\delta)$$

for an array of finite positive constants $\{c_{n,i} : i \in \mathcal{D}_n; n \geq 1\}$ and some function $\varphi(\delta) \geq 0$ with $\varphi(\delta) \rightarrow 0$ as $\delta \rightarrow \infty$, where $\mathcal{F}_{n,i}(\delta)$ is the σ -field generated by $\{e_{n,j} : \Delta(i,j) \leq \delta\}$. The $c_{n,i}$'s and $\varphi(\delta)$ are called the NED scaling factors and NED coefficient, respectively. The \mathbf{x} is said to be uniformly L^p -NED on \mathbf{e} if $c_{n,i}$ is uniformly bounded. If $\varphi(\delta) \lesssim \rho^\delta$ for some $0 < \rho < 1$, then it is called geometrically L^p -NED.

Lemma A.1. Suppose that Assumptions 2.1, 3.1, 3.2(i), and 3.3(i) hold. Then, for a given $s \in (0, 1)$, $\{q_i(s) : i \in \mathcal{D}_n; n \geq 1\}$ is uniformly and geometrically L^p -NED on $\{\varepsilon_i : i \in \mathcal{D}_n; n \geq 1\}$.

Proof. We prove the lemma in a similar manner to Jenish (2012) and Hoshino (2022). First, note that Q is uniquely determined in $\mathcal{H}_{n,\infty}$ as $Q = (\text{Id} - \mathcal{T})^{-1}X\beta_0 + (\text{Id} - \mathcal{T})^{-1}\mathcal{E}$ under Assumption 2.1. We denote the i -th element of $(\text{Id} - \mathcal{T})^{-1}X\beta_0 + (\text{Id} - \mathcal{T})^{-1}[\cdot]$ as $f_i[\cdot]$, such that $q_i = f_i[\mathcal{E}]$ holds for each $i = 1, \dots, n$.

Define

$$\mathcal{E}_{1,i}^{(\delta)} := \{\varepsilon_j\}_{j:\Delta(i,j) \leq \delta}, \quad \mathcal{E}_{2,i}^{(\delta)} := \{\varepsilon_j\}_{j:\Delta(i,j) > \delta}$$

for some $\delta > 0$. Since $L^p(0, 1)$ is separable for $1 \leq p < \infty$, under Assumption 3.3(i), both $\mathcal{E}_{1,i}^{(\delta)}$ and $\mathcal{E}_{2,i}^{(\delta)}$ are Polish space-valued random elements in $(\mathcal{H}_{\{|j:\Delta(i,j) \leq \delta\}, p}, \|\cdot\|_{\infty, p})$ and $(\mathcal{H}_{\{|j:\Delta(i,j) > \delta\}, p}, \|\cdot\|_{\infty, p})$, respectively (recall: $\mathcal{H}_{n,p} := \{H = (h_1, \dots, h_n) : h_i \in L^p(0, 1) \text{ for all } i\}$). Then, by Lemma 2.11 of Dudley and Philipp (1983) (see also Lemma A.1 of Jenish (2012)), a function χ exists such that $(\mathcal{E}_{1,i}^{(\delta)}, \chi(U, \mathcal{E}_{1,i}^{(\delta)}))$ has the same law as that of $(\mathcal{E}_{1,i}^{(\delta)}, \mathcal{E}_{2,i}^{(\delta)})$, which is an appropriate rearrangement of \mathcal{E} , where U is a random variable uniformly distributed on $[0, 1]$ and independent of $\mathcal{E}_{1,i}^{(\delta)}$.

Now, write $f_i[\mathcal{E}_{1,i}^{(\delta)}, \mathcal{E}_{2,i}^{(\delta)}] \equiv f_i[\mathcal{E}]$, and define $q_i^{(\delta)} := f_i[\mathcal{E}_{1,i}^{(\delta)}, \chi(U, \mathcal{E}_{1,i}^{(\delta)})] \equiv f_i[\mathcal{E}^{(\delta)}]$ with $\mathcal{E}^{(\delta)} = (\varepsilon_1^{(\delta)}, \dots, \varepsilon_n^{(\delta)})^\top$; specifically,

$$\begin{aligned} q_i^{(\delta)}(s) &= \left\{ (\text{Id} - \mathcal{T})^{-1}[X\beta_0 + \mathcal{E}^{(\delta)}](s) \right\}_i \\ &= \sum_{j=1}^n w_{i,j} \int_0^1 q_j^{(\delta)}(t) \alpha_0(t, s) dt + x_i^\top \beta_0(s) + \varepsilon_i^{(\delta)}(s). \end{aligned}$$

By construction, we have

$$\begin{aligned} \mathbb{E}[q_i(s) \mid \mathcal{F}_{n,i}(\delta)] &= \mathbb{E}\left[f_i[\mathcal{E}_{1,i}^{(\delta)}, \mathcal{E}_{2,i}^{(\delta)}](s) \mid \mathcal{E}_{1,i}^{(\delta)} \right] \\ &= \mathbb{E}\left[f_i[\mathcal{E}_{1,i}^{(\delta)}, \chi(U, \mathcal{E}_{1,i}^{(\delta)})](s) \mid \mathcal{E}_{1,i}^{(\delta)} \right] = \mathbb{E}[q_i^{(\delta)}(s) \mid \mathcal{F}_{n,i}(\delta)], \end{aligned}$$

where $\mathcal{F}_{n,i}(\delta)$ is the σ -field generated by $\{\varepsilon_j : \Delta(i, j) \leq \delta\}$.

Here, suppose that $0 < \delta < \bar{\Delta}$, where $\bar{\Delta}$ is as provided in Assumption 3.1(ii). Then, because at least i 's own ε_i is included in $\mathcal{E}_{1,i}^{(\delta)}$, we have $\varepsilon_i \equiv \varepsilon_i^{(\delta)}$, and hence

$$q_i(s) - q_i^{(\delta)}(s) = \sum_{j=1}^n w_{i,j} \int_0^1 [q_j(t) - q_j^{(\delta)}(t)] \alpha_0(t, s) dt$$

holds. By Minkowski's inequality,

$$\begin{aligned} \|q_i(s) - q_i^{(\delta)}(s)\|_p &= \left\| \sum_{j=1}^n w_{i,j} \int_0^1 [q_j(t) - q_j^{(\delta)}(t)] \alpha_0(t, s) dt \right\|_p \\ &\leq \sum_{j=1}^n |w_{i,j}| \cdot \int_0^1 \|q_j(t) - q_j^{(\delta)}(t)\|_p |\alpha_0(t, s)| dt \\ &\leq 2\bar{\alpha}_0 \|W_n\|_\infty \max_{1 \leq j \leq n} \int_0^1 \|q_j(t)\|_p dt \leq C_p \cdot \varrho, \end{aligned}$$

where $C_p := 2 \sup_{1 \leq i \leq n; n \geq 1} \int_0^1 \|q_i(t)\|_p dt$, and $\varrho := \bar{\alpha}_0 \|W_n\|_\infty$. Similarly, when $\bar{\Delta} \leq \delta < 2\bar{\Delta}$ holds, noting now that under Assumption 3.1(ii) we have $\varepsilon_j \equiv \varepsilon_j^{(\delta)}$ for all j 's who are direct neighbors of i ,

$$\begin{aligned} \|q_i(s) - q_i^{(\delta)}(s)\|_p &\leq \bar{\alpha}_0 \sum_{j=1}^n |w_{i,j}| \cdot \int_0^1 \|q_j(t_1) - q_j^{(\delta)}(t_1)\|_p dt_1 \\ &= \bar{\alpha}_0 \sum_{j=1}^n |w_{i,j}| \cdot \int_0^1 \left\| \sum_{k=1}^n w_{j,k} \int_0^1 [q_k(t_2) - q_k^{(\delta)}(t_2)] \alpha_0(t_2, t_1) dt_2 \right\|_p dt_1 \\ &= \bar{\alpha}_0^2 \sum_{j=1}^n |w_{i,j}| \sum_{k=1}^n |w_{j,k}| \cdot \int_0^1 \int_0^1 \|q_k(t_2) - q_k^{(\delta)}(t_2)\|_p dt_2 dt_1 \leq C_p \cdot \varrho^2. \end{aligned}$$

Applying the same argument recursively, for $m\bar{\Delta} \leq \delta < (m+1)\bar{\Delta}$ such that $\varepsilon_j \equiv \varepsilon_j^{(\delta)}$ for all j 's in the m -th order neighborhood of i , we obtain

$$\|q_i(s) - q_i^{(\delta)}(s)\|_p \leq C_p \cdot \varrho^{|\delta/\bar{\Delta}|+1}. \quad (\text{A.1})$$

Finally, by Jensen's inequality and (A.1),

$$\begin{aligned} \|q_i(s) - \mathbb{E}[q_i(s) \mid \mathcal{F}_{n,i}(\delta)]\|_p &= \left\| \int_0^1 [f_i[\mathcal{E}_{1,i}^{(\delta)}, \mathcal{E}_{2,i}^{(\delta)}](s) - f_i[\mathcal{E}_{1,i}^{(\delta)}, \chi(u, \mathcal{E}_{1,i}^{(\delta)})](s)] du \right\|_p \\ &\leq \left\{ \mathbb{E} \int_0^1 |f_i[\mathcal{E}_{1,i}^{(\delta)}, \mathcal{E}_{2,i}^{(\delta)}](s) - f_i[\mathcal{E}_{1,i}^{(\delta)}, \chi(u, \mathcal{E}_{1,i}^{(\delta)})](s)|^p du \right\}^{1/p} \\ &= \left\{ \mathbb{E} |f_i[\mathcal{E}_{1,i}^{(\delta)}, \mathcal{E}_{2,i}^{(\delta)}](s) - f_i[\mathcal{E}_{1,i}^{(\delta)}, \chi(U, \mathcal{E}_{1,i}^{(\delta)})](s)|^p \right\}^{1/p} \\ &= \|f_i[\mathcal{E}_{1,i}^{(\delta)}, \mathcal{E}_{2,i}^{(\delta)}](s) - f_i[\mathcal{E}_{1,i}^{(\delta)}, \chi(U, \mathcal{E}_{1,i}^{(\delta)})](s)\|_p \\ &= \|q_i(s) - q_i^{(\delta)}(s)\|_p \leq C_p \cdot \varrho^{|\delta/\bar{\Delta}|+1} \rightarrow 0 \end{aligned}$$

as $\delta \rightarrow \infty$ by Assumption 2.1. This completes the proof. \square

Lemma A.2. Suppose that $\{x_{n,i} : i \in \mathcal{D}_n; n \geq 1\}$ is geometrically L^2 -NED on $\{\varepsilon_i : i \in \mathcal{D}_n; n \geq 1\}$. Then, under Assumption 3.3(ii), $|\text{Cov}(x_{n,i}, x_{n,j})| \leq 32(\max_{1 \leq i \leq n} \|x_{n,i}\|_2)^2 \varphi(\Delta(i, j)/3)$ for some geometric NED coefficient φ .

Proof. Decompose $x_{n,i} = x_{n,1,i}^{(\delta)} + x_{n,2,i}^{(\delta)}$, where

$$x_{n,1,i}^{(\delta)} := \mathbb{E}[x_{n,i} | \mathcal{F}_{n,i}(\delta)], \text{ and } x_{n,2,i}^{(\delta)} := x_{n,i} - \mathbb{E}[x_{n,i} | \mathcal{F}_{n,i}(\delta)].$$

Then, for each pair $x_{n,i}$ and $x_{n,j}$, setting: $\delta = \Delta(i, j)/3$,

$$\begin{aligned} |\text{Cov}(x_{n,i}, x_{n,j})| &= \left| \text{Cov} \left(x_{n,1,i}^{(\Delta(i,j)/3)} + x_{n,2,i}^{(\Delta(i,j)/3)}, x_{n,1,j}^{(\Delta(i,j)/3)} + x_{n,2,j}^{(\Delta(i,j)/3)} \right) \right| \\ &\leq \left| \text{Cov} \left(x_{n,1,i}^{(\Delta(i,j)/3)}, x_{n,1,j}^{(\Delta(i,j)/3)} \right) \right| + \left| \text{Cov} \left(x_{n,1,i}^{(\Delta(i,j)/3)}, x_{n,2,j}^{(\Delta(i,j)/3)} \right) \right| \\ &\quad + \left| \text{Cov} \left(x_{n,2,i}^{(\Delta(i,j)/3)}, x_{n,1,j}^{(\Delta(i,j)/3)} \right) \right| + \left| \text{Cov} \left(x_{n,2,i}^{(\Delta(i,j)/3)}, x_{n,2,j}^{(\Delta(i,j)/3)} \right) \right|. \end{aligned}$$

Since $\{\varepsilon_k : \Delta(i, k) \leq \Delta(i, j)/3\}$ and $\{\varepsilon_k : \Delta(j, k) \leq \Delta(i, j)/3\}$ do not overlap, the first term on the right-hand side is zero by Assumption 3.3(ii). Note that, by Jensen's inequality, $\|x_{n,1,i}^{(\Delta(i,j)/3)}\|_2 \leq \|x_{n,i}\|_2$. In addition, $\|x_{n,2,i}^{(\Delta(i,j)/3)}\|_2 \leq 2\|x_{n,i}\|_2$. Then, since $\{x_{n,i}\}$ is assumed to be L^2 -NED, it holds that

$$\left\| x_{n,2,i}^{(\Delta(i,j)/3)} \right\|_2 = \|x_{n,i} - \mathbb{E}[x_{n,i} | \mathcal{F}_{n,i}(\Delta(i, j)/3)]\|_2 \leq 2 \max_{1 \leq i \leq n} \|x_{n,i}\|_2 \varphi(\Delta(i, j)/3).$$

Hence, Cauchy–Schwarz inequality gives

$$\left| \text{Cov} \left(x_{n,1,i}^{(\Delta(i,j)/3)}, x_{n,2,j}^{(\Delta(i,j)/3)} \right) \right| \leq 4 \left\| x_{n,1,i}^{(\Delta(i,j)/3)} \right\|_2 \left\| x_{n,2,j}^{(\Delta(i,j)/3)} \right\|_2 \leq 8 \left(\max_{1 \leq i \leq n} \|x_{n,i}\|_2 \right)^2 \varphi(\Delta(i, j)/3).$$

Similarly,

$$\left| \text{Cov} \left(x_{n,2,i}^{(\Delta(i,j)/3)}, x_{n,2,j}^{(\Delta(i,j)/3)} \right) \right| \leq 4 \left\| x_{n,2,i}^{(\Delta(i,j)/3)} \right\|_2 \left\| x_{n,2,j}^{(\Delta(i,j)/3)} \right\|_2 \leq 16 \left(\max_{1 \leq i \leq n} \|x_{n,i}\|_2 \right)^2 \varphi(\Delta(i, j)/3).$$

This completes the proof. \square

Lemma A.3. Suppose that Assumptions 2.1, 3.1, 3.2(i), 3.3(i)–(ii), and 3.4(i) hold. Then,

$$(i) \quad \left\| Z^\top \bar{R}/n - \mathbb{E}(Z^\top \bar{R}/n) \right\| \lesssim_p \frac{\sqrt{KL}}{\sqrt{n}}.$$

If Assumption 3.8 additionally holds, we have

$$(ii) \quad \left\| Z^\top \hat{R}/n - \mathbb{E}(Z^\top \bar{R}/n) \right\| \lesssim_p \frac{\sqrt{KL}}{\sqrt{n}} + \kappa^\varepsilon \sqrt{KL}.$$

Proof. (i) Write $z_i = (z_{1,i}^\top, x_i^\top)^\top = (z_{i,1}, \dots, z_{i,L+d_x})^\top$. By Assumption 3.2(i),

$$\begin{aligned}
\mathbb{E} \left\| \frac{1}{n} \sum_{i=1}^n (z_i \bar{r}_i^\top - \mathbb{E}(z_i \bar{r}_i^\top)) \right\|^2 &= \frac{1}{n^2} \sum_{k=1}^K \sum_{l=1}^{L+d_x} \mathbb{E} \left\{ \sum_{i=1}^n (z_{i,l} \bar{r}_{i,k} - \mathbb{E}(z_{i,l} \bar{r}_{i,k})) \right\}^2 \\
&= \frac{1}{n^2} \sum_{k=1}^K \sum_{l=1}^{L+d_x} \sum_{i=1}^n \text{Var}(z_{i,l} \bar{r}_{i,k}) \\
&\quad + \frac{1}{n^2} \sum_{k=1}^K \sum_{l=1}^{L+d_x} \sum_{i=1}^n \sum_{j \neq i}^n \text{Cov}(z_{i,l} \bar{r}_{i,k}, z_{j,l} \bar{r}_{j,k}) \\
&\lesssim \frac{L}{n^2} \sum_{k=1}^K \sum_{i=1}^n \mathbb{E}[\bar{r}_{i,k}^2] + \frac{L}{n^2} \sum_{k=1}^K \sum_{i=1}^n \sum_{j \neq i}^n |\text{Cov}(\bar{r}_{i,k}, \bar{r}_{j,k})|.
\end{aligned} \tag{A.2}$$

By Cauchy–Schwarz inequality, $|\int_0^1 q_i(s) \phi_k(s) ds| \leq \|q_i\|_{L^2} \|\phi_k\|_{L^2} < \infty$ by Assumption 3.4(i). Thus,

$$\mathbb{E}[\bar{r}_{i,k}^2] = \sum_{l=1}^n \sum_{j=1}^n w_{i,j} w_{i,l} \mathbb{E} \left[\int_0^1 q_j(s_1) \phi_k(s_1) ds_1 \int_0^1 q_l(s_2) \phi_k(s_2) ds_2 \right] < \infty \tag{A.3}$$

uniformly in i , implying that the first term on the right-hand side of (A.2) is of order KL/n .

Next, by Lemma A.1 as $\delta \rightarrow \infty$,

$$\begin{aligned}
\|\bar{r}_{i,k} - \mathbb{E}[\bar{r}_{i,k} | \mathcal{F}_{n,i}(\delta)]\|_2 &= \left\| \sum_{j=1}^n w_{i,j} \int_0^1 q_j(t) \phi_k(t) dt - \sum_{j=1}^n w_{i,j} \int_0^1 \mathbb{E}[q_j(t) | \mathcal{F}_{n,i}(\delta)] \phi_k(t) dt \right\|_2 \\
&\leq \sum_{j=1}^n |w_{i,j}| \left\| \int_0^1 (q_j(t) - \mathbb{E}[q_j(t) | \mathcal{F}_{n,i}(\delta)]) \phi_k(t) dt \right\|_2 \\
&\leq \sum_{j=1}^n |w_{i,j}| \int_0^1 \|q_j(t) - \mathbb{E}[q_j(t) | \mathcal{F}_{n,i}(\delta)]\|_2 |\phi_k(t)| dt \\
&\leq \|W_n\|_\infty C_2 \cdot \int_0^1 |\phi_k(t)| dt \cdot \varrho^{|\delta/\Delta|+1} \rightarrow 0.
\end{aligned}$$

Thus, $\{\bar{r}_{i,k}\}$ is uniformly and geometrically L^2 -NED on $\{\varepsilon_i\}$, and from Lemma A.2 and (A.3), $|\text{Cov}(\bar{r}_{i,k}, \bar{r}_{j,k})| \lesssim \varphi(\Delta(i, j)/3)$, where $\varphi(\delta)$ is some geometric NED coefficient. Then, Lemma A.1(iii) of Jenish and Prucha (2009) gives

$$\begin{aligned}
\frac{1}{n} \sum_{k=1}^K \sum_{i=1}^n \sum_{j \neq i}^n |\text{Cov}(\bar{r}_{i,k}, \bar{r}_{j,k})| &\lesssim \frac{1}{n} \sum_{k=1}^K \sum_{i=1}^n \sum_{j \neq i}^n \varphi(\Delta(i, j)/3) \\
&= \frac{1}{n} \sum_{k=1}^K \sum_{i=1}^n \sum_{m=1}^{\infty} \sum_{j: \Delta(i, j) \in [m, m+1)} \varphi(\Delta(i, j)/3) \\
&\lesssim \frac{1}{n} \sum_{k=1}^K \sum_{i=1}^n \sum_{m=1}^{\infty} m^{d-1} \varphi(m) \lesssim K,
\end{aligned}$$

where the last equality holds by the geometric NED property.

Combining these results, by Markov's inequality, we have the desired result.

(ii) By the triangle inequality,

$$\left\| Z^\top \widehat{R}/n - \mathbb{E}(Z^\top \overline{R}/n) \right\| \leq \left\| Z^\top (\widehat{R} - \overline{R})/n \right\| + \underbrace{\left\| Z^\top \overline{R}/n - \mathbb{E}(Z^\top \overline{R}/n) \right\|}_{\lesssim_p \sqrt{KL}/\sqrt{n} \text{ by (i)}}.$$

For the first term on the right-hand side, observe that

$$\begin{aligned} Z^\top (\widehat{R} - \overline{R})/n &= \frac{1}{n} \sum_{i=1}^n z_i (\widehat{r}_{i,k} - \overline{r}_{i,k}) \\ &= \frac{1}{n} \sum_{i=1}^n \sum_{j=1}^n z_i w_{i,j} \int_0^1 [\widehat{q}_j(t) - q_j(t)] \phi_K(t)^\top dt, \end{aligned}$$

and hence $\left\| Z^\top (\widehat{R} - \overline{R})/n \right\| \leq \frac{1}{n} \sum_{i=1}^n \sum_{j=1}^n \|z_i\| \cdot |w_{i,j}| \cdot \left\| \int_0^1 [\widehat{q}_j(t) - q_j(t)] \phi_K(t) dt \right\|$. Here, define

$$\omega_i^*(t) = \begin{cases} 0 & \text{if } t < s_{i,1} \\ \frac{s_{i,l(t)+1}-t}{s_{i,l(t)+1}-s_{i,l(t)}} & \text{if } s_{i,1} \leq t \leq s_{i,m_i} \text{ with } t \in [s_{i,l(t)}, s_{i,l(t)+1}] \\ 1 & \text{if } t > s_{i,m_i} \end{cases}$$

such that we can write for all $t \in [0, 1]$

$$\widehat{q}_i(t) = \omega_i^*(t)[q_i(s_{i,l(t)}) - q_i(s_{i,l(t)+1})] + q_i(s_{i,l(t)+1})$$

(recall: $s_{i,0} = 0$ and $s_{i,m_i+1} = 1$). Thus, under Assumption 3.8,

$$\begin{aligned} |\widehat{q}_i(t) - q_i(t)| &\leq |\omega_i^*(t)[q_i(s_{i,l(t)}) - q_i(s_{i,l(t)+1})]| + |q_i(s_{i,l(t)+1}) - q_i(t)| \\ &\leq |s_{i,l(t)} - s_{i,l(t)+1}|^\xi + |s_{i,l(t)+1} - t|^\xi \lesssim \kappa^\xi, \end{aligned} \tag{A.4}$$

uniformly in t , leading to

$$\begin{aligned} \left\| \int_0^1 [\widehat{q}_i(t) - q_i(t)] \phi_K(t) dt \right\| &\leq \int_0^1 \|[\widehat{q}_i(t) - q_i(t)] \phi_K(t)\| dt \\ &\lesssim \kappa^\xi \int_0^1 \|\phi_K(t)\| dt \\ &\lesssim \sqrt{K} \kappa^\xi \end{aligned}$$

for all i , where the last line follows from $\int_0^1 \|\phi_K(t)\| dt = \int_0^1 \left(\sum_{k=1}^K \phi_k^2(t) \right)^{1/2} dt \leq \left(\sum_{k=1}^K \|\phi_k\|_{L^2}^2 \right)^{1/2}$. This completes the proof. \square

Lemma A.4. Suppose that Assumptions 2.1, 3.1, 3.2, 3.3(i)–(ii), 3.4(i), and 3.5 hold. Then,

$$(i) \quad \left\| \overline{R}^\top M_z \overline{R}/n - \mathbb{E} \overline{R}^\top M_z \mathbb{E} \overline{R}/n \right\| \lesssim_p \frac{\sqrt{KL}}{\sqrt{n}}$$

$$(ii) \quad \left\| \left[\bar{R}^\top M_z \bar{R} / n \right]^{-1} - \left[\mathbb{E} \bar{R}^\top M_z \mathbb{E} \bar{R} / n \right]^{-1} \right\| \lesssim_p \frac{\sqrt{KL}}{\nu_{KL}^2 \sqrt{n}}$$

If Assumption 3.8 additionally holds, we have

$$(iii) \quad \left\| \hat{R}^\top M_z \hat{R} / n - \mathbb{E} \bar{R}^\top M_z \mathbb{E} \bar{R} / n \right\| \lesssim_p \frac{\sqrt{KL}}{\sqrt{n}} + \kappa^\xi \sqrt{KL}$$

$$(iv) \quad \left\| \left[\hat{R}^\top M_z \hat{R} / n \right]^{-1} - \left[\mathbb{E} \bar{R}^\top M_z \mathbb{E} \bar{R} / n \right]^{-1} \right\| \lesssim_p \frac{\sqrt{KL}}{\nu_{KL}^2 \sqrt{n}} + \frac{\kappa^\xi \sqrt{KL}}{\nu_{KL}^2}.$$

Proof. The proofs are analogous to the proof of Lemma A.7 in Hoshino (2022), and thus are omitted. \square

Proof of Theorem 3.1

(i) Letting $U(s) = (u_1(s), \dots, u_n(s))^\top$, we write

$$Q(s) = \bar{R} \theta_0(s) + X \beta_0(s) + \mathcal{E}(s) + U(s).$$

Observe that

$$\begin{aligned} u_i(s) &= \sum_{j=1}^n w_{i,j} \left[\int_0^1 q_j(t) \alpha_0(t, s) dt - \sum_{k=1}^K r_{j,k} \theta_{0k}(s) \right] \\ &= \sum_{j=1}^n w_{i,j} \left[\int_0^1 q_j(t) \alpha_0(t, s) dt - \sum_{k=1}^K \int_0^1 q_j(t) \phi_k(t) dt \cdot \theta_{0k}(s) \right] \\ &= \sum_{j=1}^n w_{i,j} \int_0^1 q_j(t) \left\{ \alpha_0(t, s) - \sum_{k=1}^K \phi_k(t) \theta_{0k}(s) \right\} dt. \end{aligned}$$

Hence, by Cauchy–Schwarz inequality,

$$|u_i(s)| \leq \|W_n\|_\infty \cdot \max_{1 \leq i \leq n} \|q_i\|_{L^2} \cdot \left\| \alpha_0(\cdot, s) - \sum_{k=1}^K \phi_k(\cdot) \theta_{0k}(s) \right\|_{L^2} \lesssim \ell_K(s) \quad (A.5)$$

uniformly in i .

Noting that $X^\top S \bar{R} = X^\top \bar{R}$, we decompose

$$\begin{aligned} \hat{\beta}_n(s) - \beta_0(s) &= [X^\top (I_n - S) X]^{-1} X^\top (I_n - S) Q(s) - \beta_0(s) \\ &= [X^\top (I_n - S) X]^{-1} X^\top (I_n - S) [\bar{R} \theta_0(s) + \mathcal{E}(s) + U(s)] \\ &= [X^\top (I_n - S) X]^{-1} X^\top (I_n - S) \mathcal{E}(s) + [X^\top (I_n - S) X]^{-1} X^\top (I_n - S) U(s) \\ &=: A_1 + A_2, \text{ say.} \end{aligned}$$

By a straightforward matrix-norm calculation (see, e.g., Fact A.2 in Hoshino (2022)) and Lemmas

A.3(i) and A.4(ii)

$$\begin{aligned}
& \left\| X^\top S X/n - \mathbb{E}(X^\top \bar{R}/n) \left[\mathbb{E} \bar{R}^\top M_z \mathbb{E} \bar{R}/n \right]^{-1} \mathbb{E}(\bar{R}^\top X/n) \right\| \\
& \lesssim \rho_{\max} \left((\bar{R}^\top X/n)(X^\top \bar{R}/n) \right) \left\| \left[\bar{R}^\top M_z \bar{R}/n \right]^{-1} - \left[\mathbb{E} \bar{R}^\top M_z \mathbb{E} \bar{R}/n \right]^{-1} \right\| \\
& \quad + \rho_{\max} \left(\left[\mathbb{E} \bar{R}^\top M_z \mathbb{E} \bar{R}/n \right]^{-1} \right) \left\| \bar{R}^\top X/n - \mathbb{E}(\bar{R}^\top X/n) \right\| \lesssim_p \frac{\sqrt{KL}}{\nu_{KL}^2 \sqrt{n}} + \frac{\sqrt{K}}{\nu_{KL} \sqrt{n}}.
\end{aligned}$$

This implies that

$$\|X^\top (I_n - S)X/n - \Sigma_{n,x}\| \lesssim_p \frac{\sqrt{KL}}{\nu_{KL}^2 \sqrt{n}} \rightarrow 0, \tag{A.6}$$

where recall that

$$\Sigma_{n,x} = X^\top X/n - \mathbb{E}(X^\top \bar{R}/n) \left[\mathbb{E} \bar{R}^\top M_z \mathbb{E} \bar{R}/n \right]^{-1} \mathbb{E}(\bar{R}^\top X/n).$$

Under Assumption 3.6, (A.6) ensures that $\rho_{\min}(X^\top (I_n - S)X/n) > 0$ with probability approaching one. Because the eigenvalue of an idempotent matrix is at most one, we obtain by (A.5) that

$$\begin{aligned}
\|A_2\|^2 &= U(s)^\top (I_n - S)X \left[X^\top (I_n - S)X \right]^{-2} X^\top (I_n - S)U(s) \\
&\lesssim_p U(s)^\top (I_n - S)X \left[X^\top (I_n - S)X \right]^{-1} X^\top (I_n - S)U(s)/n \\
&\lesssim_p \frac{1}{n} \sum_{i=1}^n |u_i(s)|^2 \lesssim \ell_K^2(s).
\end{aligned}$$

Hence, $\|A_2\| \lesssim_p \ell_K(s)$.

Next, for A_1 , decompose $A_1 := A_{11} + A_{12}$, where

$$\begin{aligned}
A_{11} &:= \Sigma_{n,x}^{-1} \Psi_{n,x}^\top \mathcal{E}(s)/n \\
A_{12} &:= \left[X^\top (I_n - S)X/n \right]^{-1} X^\top (I_n - S)\mathcal{E}(s)/n - \Sigma_{n,x}^{-1} \Psi_{n,x}^\top \mathcal{E}(s)/n
\end{aligned}$$

and recall that

$$\Psi_{n,x} = X - \mathbb{E}(M_z \bar{R}/n) \left[\mathbb{E} \bar{R}^\top M_z \mathbb{E} \bar{R}/n \right]^{-1} \mathbb{E}(\bar{R}^\top X/n).$$

By Assumptions 3.3(ii) and 3.6, $\mathbb{E}\|A_{11}\|^2 = \text{tr} \{ \Sigma_{n,x}^{-1} \Omega_{n,x} \Sigma_{n,x}^{-1} \} / n \lesssim 1/n$. Hence, it follows from Markov's inequality that $\|A_{11}\| \lesssim_p n^{-1/2}$.

Next, let

$$\begin{aligned}
\mathcal{P} &:= (Z^\top Z/n)^- \mathbb{E}(Z^\top \bar{R}/n) \left[\mathbb{E} \bar{R}^\top M_z \mathbb{E} \bar{R}/n \right]^{-1} \mathbb{E}(\bar{R}^\top Z/n) (Z^\top Z/n)^- \\
\hat{\mathcal{P}} &:= (Z^\top Z/n)^- (Z^\top \bar{R}/n) \left[\bar{R}^\top M_z \bar{R}/n \right]^{-1} (\bar{R}^\top Z/n) (Z^\top Z/n)^-
\end{aligned}$$

such that we can write $X^\top(I_n - S)\mathcal{E}(s)/n = X^\top\mathcal{E}(s)/n - (X^\top Z/n)\widehat{\mathcal{P}}(Z^\top\mathcal{E}(s)/n)$ and $\Psi_{n,x}^\top\mathcal{E}(s)/n = X^\top\mathcal{E}(s)/n - (X^\top Z/n)\mathcal{P}(Z^\top\mathcal{E}(s)/n)$. A_{12} can be decomposed further into three terms in the following manner:

$$\begin{aligned} A_{12} &= \left\{ [X^\top(I_n - S)X/n]^{-1} - \Sigma_{n,x}^{-1} \right\} X^\top\mathcal{E}(s)/n \\ &\quad - \left\{ [X^\top(I_n - S)X/n]^{-1} - \Sigma_{n,x}^{-1} \right\} (X^\top Z/n)\widehat{\mathcal{P}}(Z^\top\mathcal{E}(s)/n) - \Sigma_{n,x}^{-1}(X^\top Z/n)\{\widehat{\mathcal{P}} - \mathcal{P}\}(Z^\top\mathcal{E}(s)/n) \\ &=: A_{12a} - A_{12b} - A_{12c}, \text{ say.} \end{aligned}$$

By Markov's inequality, it is easy to observe $\|X^\top\mathcal{E}(s)/n\| \lesssim_p n^{-1/2}$. Then, by (A.6) and Assumption 3.6, we have $\|A_{12a}\| \lesssim_p \sqrt{KL}/(\nu_{KL}^2 n)$. Similarly, for A_{12b} , noting that $\rho_{\max}(\widehat{\mathcal{P}}) \leq \rho_{\max}((Z^\top Z/n)^-) \lesssim 1$,

$$\begin{aligned} \|A_{12b}\|^2 &\lesssim_p \frac{KL}{\nu_{KL}^4 n} \cdot \text{tr} \left\{ (X^\top Z/n)\widehat{\mathcal{P}}(Z^\top\mathcal{E}(s)/n)(\mathcal{E}(s)^\top Z/n)\widehat{\mathcal{P}}(Z^\top X/n) \right\} \\ &\lesssim_p \frac{KL}{\nu_{KL}^4 n} \cdot \|(X^\top Z/n)(Z^\top\mathcal{E}(s)/n)\|^2. \end{aligned}$$

Hence, it also holds that $\|A_{12b}\| \lesssim_p \sqrt{KL}/(\nu_{KL}^2 n)$ by Assumptions 3.3(ii) and (iii).

Here, note that

$$\|\widehat{\mathcal{P}} - \mathcal{P}\| \lesssim_p \frac{\sqrt{KL}}{\nu_{KL}^2 \sqrt{n}}$$

by Lemmas A.3(i) and A.4(ii). Thus, for A_{12c} , we have

$$\|A_{12c}\|^2 \lesssim \left\| \Sigma_{n,x}^{-1}(X^\top Z/n)\{\widehat{\mathcal{P}} - \mathcal{P}\} \right\|^2 \cdot \|Z^\top\mathcal{E}(s)/n\|^2$$

implying that $\|A_{12c}\| \lesssim_p L\sqrt{K}/(\nu_{KL}^2 n)$. Combining these results, we obtain the desired result under $L\sqrt{K}/(\nu_{KL}^2 \sqrt{n}) \lesssim 1$.

(ii) Note that $\overline{R}_x^\top M_z \overline{R}_x/n = \overline{R}^\top (M_z - M_x)\overline{R}/n$. Then,

$$\begin{aligned} \left\| \overline{R}_x^\top M_z \overline{R}_x/n - \mathbb{E}\overline{R}_x^\top M_z \mathbb{E}\overline{R}_x \right\| &\leq \left\| \overline{R}^\top M_z \overline{R}/n - \mathbb{E}\overline{R}^\top M_z \mathbb{E}\overline{R}/n \right\| \\ &\quad + \left\| \overline{R}^\top M_x \overline{R}/n - \mathbb{E}\overline{R}^\top M_x \mathbb{E}\overline{R}/n \right\| = o_P(1) \end{aligned}$$

by Lemma A.4(i). With this, Assumption 3.5(ii) implies that $\rho_{\min}(\overline{R}_x^\top M_z \overline{R}_x/n) \geq c\nu_{KL}$ with probability approaching one for some $1 > c > 0$. Thus, by Weyl's inequality,

$$\rho_{\min} \left(\overline{R}_x^\top M_z \overline{R}_x/n + \lambda Dn \right) \geq c[\nu_{KL} + \lambda \rho_D]$$

with probability approaching one. Now, decompose

$$\widehat{\theta}_n(s) - \theta_0(s) = \left[\overline{R}_x^\top M_z \overline{R}_x + \lambda Dn \right]^{-1} \overline{R}_x^\top M_z Q(s) - \theta_0(s)$$

$$\begin{aligned}
&= \left[\overline{R}_x^\top M_z \overline{R}_x + \lambda D n \right]^{-1} \overline{R}_x^\top M_z \overline{R} \theta_0(s) - \theta_0(s) \\
&\quad + \left[\overline{R}_x^\top M_z \overline{R}_x + \lambda D n \right]^{-1} \overline{R}_x^\top M_z \mathcal{E}(s) + \left[\overline{R}_x^\top M_z \overline{R}_x + \lambda D n \right]^{-1} \overline{R}_x^\top M_z U(s) \\
&=: B_1 + B_2 + B_3, \text{ say.}
\end{aligned}$$

Noting that $R_x^\top M_z \overline{R}_x = R_x^\top M_z \overline{R}$ and

$$\begin{aligned}
B_1 &= \left[\overline{R}_x^\top M_z \overline{R}_x + \lambda D n \right]^{-1} \left[\overline{R}_x^\top M_z \overline{R} + \lambda D n - \lambda D n \right] \theta_0(s) - \theta_0(s) \\
&= -\lambda \widehat{\Sigma}_{n,r,\lambda}^{-1} D \theta_0(s),
\end{aligned}$$

where $\widehat{\Sigma}_{n,r,\lambda} := \overline{R}_x^\top M_z \overline{R}_x / n + \lambda D$,

$$\|B_1\|^2 = \lambda^2 \cdot \theta_0(s)^\top D \widehat{\Sigma}_{n,r,\lambda}^{-2} D \theta_0(s) \lesssim_p \frac{\lambda^2 \|\theta_0(s)\|_D^2}{(\nu_{KL} + \lambda \rho_D)^2}.$$

Here, for any matrices A and B such that $A^\top A$ is nonsingular and B is symmetric and positive semidefinite, it holds that¹

$$\begin{aligned}
A[A^\top A]^{-1} A^\top - A[A^\top A + B]^{-1} A^\top &= A \left([A^\top A]^{-1} - [A^\top A + B]^{-1} \right) A^\top \\
&= A \left([A^\top A + B]^{-1} \left[(A^\top A + B) - (A^\top A) \right] [A^\top A]^{-1} \right) A^\top \\
&= A \left([A^\top A + B]^{-1} B [A^\top A]^{-1} \right) A^\top, \\
&\quad \text{symmetric positive semidefinite}
\end{aligned}$$

which implies that

$$\rho_{\max}(A[A^\top A + B]^{-1} A^\top) \leq 1. \tag{A.7}$$

From this with $A = M_z \overline{R}_x / \sqrt{n}$ and $B = \lambda D$, we can easily observe that $\|B_3\| \lesssim_p \ell_K(s) / \sqrt{\nu_{KL} + \lambda \rho_D}$. For B_2 , decompose $B_2 := B_{21} + B_{22} + B_{23}$, where

$$\begin{aligned}
B_{21} &:= \Sigma_{n,r,\lambda}^{-1} \mathbb{E} \overline{R}_x^\top M_z \mathcal{E}(s) / n \\
B_{22} &:= \left\{ \widehat{\Sigma}_{n,r,\lambda}^{-1} - \Sigma_{n,r,\lambda}^{-1} \right\} \mathbb{E} \overline{R}_x^\top M_z \mathcal{E}(s) / n \\
B_{23} &:= \widehat{\Sigma}_{n,r,\lambda}^{-1} \left\{ \overline{R}_x - \mathbb{E} \overline{R}_x \right\}^\top M_z \mathcal{E}(s) / n.
\end{aligned}$$

Note that (A.7) implies the following:

$$\begin{aligned}
\rho_{\max} \left([A^\top A + B]^{-1} A^\top A [A^\top A + B]^{-1} \right) &= \rho_{\max} \left([A^\top A + B]^{-1} A^\top A (A^\top A)^{-1} A^\top A [A^\top A + B]^{-1} \right) \\
&= \rho_{\max} \left((A^\top A)^{-1/2} A^\top A [A^\top A + B]^{-2} A^\top A (A^\top A)^{-1/2} \right) \tag{A.8} \\
&\leq \rho_{\max} \left([A^\top A + B]^{-1} \right).
\end{aligned}$$

Using this, we obtain $\|B_{21}\| \lesssim_p \sqrt{K} / \sqrt{n(\nu_{KL} + \lambda \rho_D)}$. Next, by the same argument as in Lemma

¹The symmetricity can be confirmed by $A \left([A^\top A + B]^{-1} B [A^\top A]^{-1} \right) A^\top = A \left([A^\top A]^{-1} B [A^\top A + B]^{-1} \right) A^\top$.

A.4(ii), we have

$$\left\| \widehat{\Sigma}_{n,r,\lambda}^{-1} - \Sigma_{n,r,\lambda}^{-1} \right\| \lesssim_p \frac{\sqrt{KL}}{\sqrt{n}(\nu_{KL} + \lambda\rho_D)^2} \rightarrow 0.$$

Thus, by Markov's inequality, $\|B_{22}\| = o_P(\sqrt{K}/\sqrt{n})$. Finally, it is straightforward to observe that

$$\begin{aligned} \|B_{23}\| &\leq \left\| \widehat{\Sigma}_{n,r,\lambda}^{-1} \left\{ \overline{R}_x^\top Z/n - \mathbb{E} \overline{R}_x^\top Z/n \right\} \right\| \cdot \left\| (Z^\top Z/n)^{-1} Z^\top \mathcal{E}(s)/n \right\| \\ &\lesssim_p \left(\frac{\sqrt{KL}}{\sqrt{n}(\nu_{KL} + \lambda\rho_D)} \right) \cdot \left(\frac{\sqrt{L}}{\sqrt{n}} \right) = o \left(\frac{\sqrt{K}}{\sqrt{n}(\nu_{KL} + \lambda\rho_D)} \right) \end{aligned}$$

by Lemma A.3(i), where the last equality is due to $L/\sqrt{n(\nu_{KL} + \lambda\rho_D)} = o(1)$. Combining these results, we obtain

$$\left\| \widehat{\theta}_n(s) - \theta_0(s) \right\| \lesssim_p \frac{\sqrt{K}/\sqrt{n} + \ell_K(s)}{\sqrt{\nu_{KL} + \lambda\rho_D}} + \frac{\lambda \|\theta_0(s)\|_D}{\nu_{KL} + \lambda\rho_D}. \quad (\text{A.9})$$

By the triangle inequality,

$$\begin{aligned} \|\widehat{\alpha}_n(\cdot, s) - \alpha_0(\cdot, s)\|_{L^2} &\leq \|\phi_K(\cdot)^\top \theta_0(s) - \alpha_0(\cdot, s)\|_{L^2} + \|\phi_K(\cdot)^\top (\widehat{\theta}_n(s) - \theta_0(s))\|_{L^2} \\ &\lesssim \ell_K(s) + \|\phi_K(\cdot)^\top (\widehat{\theta}_n(s) - \theta_0(s))\|_{L^2}. \end{aligned}$$

Under Assumption 3.4(iii), we have

$$\begin{aligned} \|\phi_K(\cdot)^\top (\widehat{\theta}_n(s) - \theta_0(s))\|_{L^2}^2 &= (\widehat{\theta}_n(s) - \theta_0(s))^\top \left\{ \int_0^1 \phi_K(t) \phi_K(t)^\top dt \right\} (\widehat{\theta}_n(s) - \theta_0(s)) \\ &\lesssim \|\widehat{\theta}_n(s) - \theta_0(s)\|_{L^2}^2. \end{aligned}$$

Then, the proof is completed in view of (A.9). \square

Proof of Theorem 3.2

(i) Using the notation in the proof of Theorem 3.1(i), we have $\sqrt{n}(\widehat{\beta}_n(s) - \beta_0(s)) = \sqrt{n}A_1 + \sqrt{n}A_2$. Recalling that $\|A_2\| \lesssim_p \ell_K(s)$, $\sqrt{n}A_2 = o_P(1)$ holds by assumption. Further, as shown in the proof of Theorem 3.1(i), $A_1 = A_{11} + A_{12a} - A_{12b} - A_{12c}$ with

$$\|A_{12a}\| \lesssim_p \frac{\sqrt{KL}}{\nu_{KL}^2 n}, \quad \|A_{12b}\| \lesssim_p \frac{\sqrt{KL}}{\nu_{KL}^2 n}, \quad \|A_{12c}\| \lesssim_p \frac{L\sqrt{K}}{\nu_{KL}^2 n}.$$

Hence, $\sqrt{n}A_1 = \sqrt{n}A_{11} + o_P(1)$ under the assumptions made here. Here, let \mathbf{c} be an arbitrary $d_x \times 1$ vector such that $\|\mathbf{c}\| = 1$, and let

$$a_n := \mathbf{c}^\top \Lambda_{n,x}^{-1/2} \underbrace{\Sigma_{n,x}^{-1} \Psi_{n,x}^\top \mathcal{E}_n(s)}_{\sqrt{n}A_{11}} / \sqrt{n},$$

where $\Lambda_{n,x} := \Sigma_{n,x}^{-1} \Omega_{n,x} \Sigma_{n,x}^{-1}$. Below, we show that

$$a_n \xrightarrow{d} \mathcal{N}(0, 1),$$

which implies the desired result. Define

$$\tilde{a}_{n,i} := n^{-1/2} \mathbf{c}^\top \Lambda_{n,x}^{-1/2} \Sigma_{n,x}^{-1} (x_i - \tilde{z}_i) \varepsilon_i(s),$$

where $\tilde{z}_i := (X^\top Z/n) \mathcal{P} z_i$. Then, $a_n = \sum_{i=1}^n \tilde{a}_{n,i}$ holds with $\mathbb{E} \tilde{a}_{n,i} = 0$ and $\sum_{i=1}^n \mathbb{E}(\tilde{a}_{n,i}^2) = 1$. Letting $\tilde{a}_{n,1,i} := n^{-1/2} \mathbf{c}^\top \Lambda_{n,x}^{-1/2} \Sigma_{n,x}^{-1} x_i \varepsilon_i(s)$ and $\tilde{a}_{n,2,i} := -n^{-1/2} \mathbf{c}^\top \Lambda_{n,x}^{-1/2} \Sigma_{n,x}^{-1} \tilde{z}_i \varepsilon_i(s)$ so that $\tilde{a}_{n,i} = \tilde{a}_{n,1,i} + \tilde{a}_{n,2,i}$, by the c_r -inequality, $\mathbb{E}(\tilde{a}_{n,i}^4) \leq 8\mathbb{E}(\tilde{a}_{n,1,i}^4) + 8\mathbb{E}(\tilde{a}_{n,2,i}^4)$ holds, where

$$\mathbb{E}(\tilde{a}_{n,1,i}^4) \lesssim n^{-2} \mathbf{c}^\top \Lambda_{n,x}^{-1/2} \Sigma_{n,x}^{-1} x_i x_i^\top \Sigma_{n,x}^{-1} \Lambda_{n,x}^{-1/2} \mathbf{c} \mathbf{c}^\top \Lambda_{n,x}^{-1/2} \Sigma_{n,x}^{-1} x_i x_i^\top \Sigma_{n,x}^{-1} \Lambda_{n,x}^{-1/2} \mathbf{c} \lesssim n^{-2},$$

and

$$\mathbb{E}(\tilde{a}_{n,2,i}^4) \lesssim n^{-2} \mathbf{c}^\top \Lambda_{n,x}^{-1/2} \Sigma_{n,x}^{-1} \tilde{z}_i \tilde{z}_i^\top \Sigma_{n,x}^{-1} \Lambda_{n,x}^{-1/2} \mathbf{c} \mathbf{c}^\top \Lambda_{n,x}^{-1/2} \Sigma_{n,x}^{-1} \tilde{z}_i \tilde{z}_i^\top \Sigma_{n,x}^{-1} \Lambda_{n,x}^{-1/2} \mathbf{c} \lesssim n^{-2} \|\tilde{z}_i\|^4 \lesssim L^2/n^2$$

under Assumption 3.3(iii). Hence, $\sum_{i=1}^n \mathbb{E}(\tilde{a}_{n,i}^4) \lesssim L^2/n \rightarrow 0$. Then, applying Lyapunov's central limit theorem completes the proof.

(ii) First, by Weyl's inequality,

$$\begin{aligned} \rho_{\min}([A^\top A + B]^{-1} A^\top A [A^\top A + B]^{-1}) &= \rho_{\min}([A^\top A + B]^{-1} - [A^\top A + B]^{-1} B [A^\top A + B]^{-1}) \\ &\geq \rho_{\min}([A^\top A + B]^{-1}) - \rho_{\max}([A^\top A + B]^{-1} B [A^\top A + B]^{-1}). \end{aligned} \quad (\text{A.10})$$

Then, setting $A = M_z \mathbb{E} \bar{R}_x / \sqrt{n}$ and $B = \lambda D$, by Assumption 3.3(iii) we have

$$\begin{aligned} [\sigma_{n,\lambda}(t, s)]^2 &= \phi_K(t)^\top \Sigma_{n,r,\lambda}^{-1} \Omega_{n,r}(s) \Sigma_{n,r,\lambda}^{-1} \phi_K(t) \\ &\geq c_1 \cdot \phi_K(t)^\top \left[\mathbb{E} \bar{R}_x^\top M_z \mathbb{E} \bar{R}_x / n + \lambda D \right]^{-1} \left(\mathbb{E} \bar{R}_x^\top M_z \mathbb{E} \bar{R}_x / n \right) \left[\mathbb{E} \bar{R}_x^\top M_z \mathbb{E} \bar{R}_x / n + \lambda D \right]^{-1} \phi_K(t) \\ &\geq \{c_2 / (1 + \lambda) - c_3 \lambda / (\nu_{KL} + \lambda \rho_D)\} \cdot \|\phi_K(t)\|^2 \\ &\geq c_4 \cdot \|\phi_K(t)\|^2 \end{aligned} \quad (\text{A.11})$$

for a sufficiently large n under the assumption $\lambda / \nu_{KL}^2 \rightarrow 0$, where the c_1, \dots, c_4 are some fixed constants.

We can write

$$\frac{\sqrt{n}(\hat{\alpha}_n(t, s) - \alpha_0(t, s))}{\sigma_{n,\lambda}(t, s)} = \frac{\sqrt{n} \phi_K(t)^\top (B_1 + B_{21} + B_{22} + B_{23} + B_3)}{\sigma_{n,\lambda}(t, s)} + \frac{\sqrt{n}(\phi_K(t)^\top \theta_0(s) - \alpha_0(t, s))}{\sigma_{n,\lambda}(t, s)}.$$

Recalling that

$$\|B_1\| \lesssim_p \frac{\lambda \|\theta_0(s)\|_D}{\nu_{KL} + \lambda \rho_D}, \quad \|B_{22}\| \lesssim_p \frac{K \sqrt{L}}{n(\nu_{KL} + \lambda \rho_D)^2}, \quad \|B_{23}\| \lesssim_p \frac{L \sqrt{K}}{n(\nu_{KL} + \lambda \rho_D)}, \quad \|B_3\| \lesssim_p \frac{\ell_K(s)}{\sqrt{\nu_{KL} + \lambda \rho_D}},$$

we can find that the dominant term of $\sqrt{n}(\hat{\alpha}_n(t, s) - \alpha_0(t, s)) / \sigma_{n,\lambda}(t, s)$ is $\sqrt{n} \phi_K(t)^\top B_{21} / \sigma_{n,\lambda}(t, s)$

considering (A.11) under the assumptions introduced here.

Let

$$b_n := [\sigma_{n,\lambda}(t, s)]^{-1} \phi_K(t)^\top \underbrace{\Sigma_{n,r,\lambda}^{-1} \mathbb{E} \bar{R}_x^\top M_z \mathcal{E}(s) / \sqrt{n}}_{\sqrt{n} B_{21}}$$

$$\tilde{b}_{n,i} := n^{-1/2} [\sigma_{n,\lambda}(t, s)]^{-1} \phi_K(t)^\top \Sigma_{n,r,\lambda}^{-1} (\mathbb{E} \bar{R}_x^\top Z/n) (Z^\top Z/n)^{-1} z_i \varepsilon_i(s)$$

such that $b_n = \sum_{i=1}^n \tilde{b}_{n,i}$, $\mathbb{E} \tilde{b}_{n,i} = 0$, and $\sum_{i=1}^n \mathbb{E}(\tilde{b}_{n,i}^2) = 1$ hold. Observe that

$$\begin{aligned} \mathbb{E}(\tilde{b}_{n,i}^4) &\lesssim \frac{1}{n^2 [\sigma_{n,\lambda}(t, s)]^4} \left(z_i^\top (Z^\top Z/n)^{-1} (Z^\top \mathbb{E} \bar{R}_x/n) \Sigma_{n,r,\lambda}^{-1} \phi_K(t) \phi_K(t)^\top \Sigma_{n,r,\lambda}^{-1} (\mathbb{E} \bar{R}_x^\top Z/n) (Z^\top Z/n)^{-1} z_i \right)^2 \\ &\lesssim \frac{1}{n^2} \left(z_i^\top (Z^\top Z/n)^{-1} (Z^\top \mathbb{E} \bar{R}_x/n) \Sigma_{n,r,\lambda}^{-2} (\mathbb{E} \bar{R}_x^\top Z/n) (Z^\top Z/n)^{-1} z_i \right)^2 \\ &\lesssim \frac{\|z_i\|^2}{n^2} z_i^\top (Z^\top Z/n)^{-1} (Z^\top \mathbb{E} \bar{R}_x/n) \Sigma_{n,r,\lambda}^{-2} (\mathbb{E} \bar{R}_x^\top M_z \mathbb{E} \bar{R}_x/n) \Sigma_{n,r,\lambda}^{-2} (\mathbb{E} \bar{R}_x^\top Z/n) (Z^\top Z/n)^{-1} z_i \\ &\lesssim \frac{\|z_i\|^2}{n^2 (\nu_{KL} + \lambda \rho_D)} z_i^\top (Z^\top Z/n)^{-1} (Z^\top \mathbb{E} \bar{R}_x/n) \Sigma_{n,r,\lambda}^{-2} (\mathbb{E} \bar{R}_x^\top Z/n) (Z^\top Z/n)^{-1} z_i \\ &\lesssim \frac{\|z_i\|^2}{n^2 (\nu_{KL} + \lambda \rho_D)^2} z_i^\top (Z^\top Z/n)^{-1} (Z^\top \mathbb{E} \bar{R}_x/n) \Sigma_{n,r,\lambda}^{-1} (\mathbb{E} \bar{R}_x^\top Z/n) (Z^\top Z/n)^{-1} z_i \\ &\lesssim \frac{\|z_i\|^2}{n^2 (\nu_{KL} + \lambda \rho_D)^2} z_i^\top (Z^\top Z/n)^{-1} z_i \\ &\lesssim \frac{L^2}{n^2 (\nu_{KL} + \lambda \rho_D)^2} \end{aligned}$$

where we have used (A.8) with $A = M_z \mathbb{E} \bar{R}_x / \sqrt{n}$ and $B = \lambda D$ in the fourth inequality and (A.7) with $A = (Z^\top Z/n)^{-1/2} (Z^\top \mathbb{E} \bar{R}_x/n)$ and $B = \lambda D$ in the sixth inequality. This suggests that $\sum_{i=1}^n \mathbb{E}(\tilde{b}_{n,i}^4) \rightarrow 0$, and the result follows from Lyapunov's central limit theorem.

(iii), (iv) We only prove that $Z^\top \widehat{\mathbf{V}}_n(s) Z/n$ converges in probability to $Z^\top \mathbf{V}_n(s) Z/n$; the consistency of $X^\top \widehat{\mathbf{V}}_n(s) X/n$ is analogous. The consistency of the other parts are already proved in the preceding arguments. Let $\tilde{\mathbf{V}}_n(s) := \text{diag}\{\varepsilon_1^2(s), \dots, \varepsilon_n^2(s)\}$. By the triangle inequality,

$$\left\| Z^\top \widehat{\mathbf{V}}_n(s) Z/n - Z^\top \mathbf{V}_n(s) Z/n \right\| \leq \left\| Z^\top \left[\widehat{\mathbf{V}}_n(s) - \tilde{\mathbf{V}}_n(s) \right] Z/n \right\| + \left\| Z^\top \left[\tilde{\mathbf{V}}_n(s) - \mathbf{V}_n(s) \right] Z/n \right\|.$$

Under Assumptions 3.3(ii) and (iii), by Markov's inequality, it is easy to observe that the second term on the right-hand side is of order L/\sqrt{n} under Assumption 3.3(iii).

Write $\widehat{\varepsilon}_i(s) = \varepsilon_i(s) + t_{n,r,i}(s) + t_{n,x,i}(s)$, where

$$t_{n,r,i}(s) := \int_0^1 \bar{q}_i(t) [\alpha_0(t, s) - \check{\alpha}_n(t, s)] dt, \quad t_{n,x,i}(s) := x_i^\top (\beta_0(s) - \hat{\beta}_n(s)),$$

where $\check{\alpha}_n(t, s) := \phi_K(t)^\top \check{\theta}_n(s)$. By Theorem 3.1(i), we have $|t_{n,x,i}(s)| \lesssim_p n^{-1/2}$ uniformly in i . For $t_{n,r,i}(s)$, noting that $|\int_0^1 \bar{q}_i(t) [\alpha_0(t, s) - \check{\alpha}_n(t, s)] dt| \lesssim \|\alpha_0(\cdot, s) - \check{\alpha}_n(\cdot, s)\|_{L^2}$ by Cauchy-Schwarz inequality, Theorem 3.1(ii) gives $|t_{n,r,i}(s)| \lesssim_p \sqrt{K}/\sqrt{n \nu_{KL}}$ uniformly in i . As $\widehat{\varepsilon}_i^2(s) - \varepsilon_i^2(s) = t_{n,r,i}^2(s) +$

$t_{n,x,i}^2(s) + 2t_{n,r,i}(s)\varepsilon_i(s) + 2t_{n,x,i}(s)\varepsilon_i(s) + 2t_{n,r,i}(s)t_{n,x,i}(s)$, we can decompose

$$Z^\top \left[\widehat{\mathbf{V}}_n(s) - \widetilde{\mathbf{V}}_n(s) \right] Z/n = \gamma_{n1} + \gamma_{n2} + 2\gamma_{n3} + 2\gamma_{n4} + 2\gamma_{n5},$$

where $\gamma_{n1} := n^{-1} \sum_{i=1}^n z_i z_i^\top t_{n,r,i}^2(s)$, $\gamma_{n2} := n^{-1} \sum_{i=1}^n z_i z_i^\top t_{n,x,i}^2(s)$, $\gamma_{n3} := n^{-1} \sum_{i=1}^n z_i z_i^\top \varepsilon_i(s) t_{n,r,i}(s)$, $\gamma_{n4} := n^{-1} \sum_{i=1}^n z_i z_i^\top \varepsilon_i(s) t_{n,x,i}(s)$, and $\gamma_{n5} := n^{-1} \sum_{i=1}^n z_i z_i^\top t_{n,r,i}(s) t_{n,x,i}(s)$. Then, by Markov's inequality, we have

$$\begin{aligned} \|\gamma_{n1}\| &\lesssim_p K\sqrt{L}/(n\nu_{KL}), & \|\gamma_{n2}\| &\lesssim_p \sqrt{L}/n, & \|\gamma_{n3}\| &\lesssim_p \sqrt{KL}/\sqrt{n\nu_{KL}} \\ \|\gamma_{n4}\| &\lesssim_p \sqrt{L}/\sqrt{n}, & \|\gamma_{n5}\| &\lesssim_p \sqrt{KL}/(n\sqrt{\nu_{KL}}). \end{aligned}$$

This completes the proof. \square

Lemma A.5. Under the assumptions made in Theorem 3.3, we have

$$\frac{nB_{21}^\top \Phi_{\mathcal{I}} B_{21} - \mu_n}{\sqrt{v_n}} \xrightarrow{d} \mathcal{N}(0, 1).$$

Proof. Recalling that $\Xi_n := \Sigma_{n,r,\lambda}^{-1} \mathbb{E}(\overline{R}_x^\top Z)(Z^\top Z)^{-}$, observe

$$\begin{aligned} \mathbb{E}[nB_{21}^\top \Phi_{\mathcal{I}} B_{21}] &= \mathbb{E}[\mathcal{E}(s)^\top Z(Z^\top Z)^{-} \mathbb{E}(Z^\top \overline{R}_x) \Sigma_{n,r,\lambda}^{-1} \Phi_{\mathcal{I}} \Sigma_{n,r,\lambda}^{-1} \mathbb{E}(\overline{R}_x^\top Z)(Z^\top Z)^{-} Z^\top \mathcal{E}(s)]/n \\ &= \text{tr} \left\{ \mathbb{E}[\Xi_n^\top \Phi_{\mathcal{I}} \Xi_n Z^\top \mathcal{E}(s) \mathcal{E}(s)^\top Z]/n \right\} \\ &= \text{tr} \left\{ \underbrace{\Xi_n^\top \Phi_{\mathcal{I}} \Xi_n (Z^\top \mathbf{V}_n(s) Z/n)}_{= \mu_n} \right\}. \end{aligned}$$

Letting $\pi_{n,i,j} := z_i^\top \Xi_n^\top \Phi_{\mathcal{I}} \Xi_n z_j$, we can write

$$\begin{aligned} nB_{21}^\top \Phi_{\mathcal{I}} B_{21} &= \frac{1}{n} \sum_{i=1}^n \sum_{j=1}^n \pi_{n,i,j} \varepsilon_i(s) \varepsilon_j(s) \\ &= \frac{2}{n} \sum_{1 \leq i < j \leq n} \pi_{n,i,j} \varepsilon_i(s) \varepsilon_j(s) + \underbrace{\frac{1}{n} \sum_{i=1}^n \pi_{n,i,i} \varepsilon_i^2(s)}_{= \text{tr} \{ \Xi_n^\top \Phi_{\mathcal{I}} \Xi_n (Z^\top \widetilde{\mathbf{V}}_n(s) Z/n) \}}. \end{aligned}$$

Here, we have

$$\begin{aligned} \|\Xi_n^\top \Phi_{\mathcal{I}} \Xi_n\|^2 &\lesssim \text{tr} \{ \Xi_n \Xi_n^\top \Xi_n \Xi_n^\top \} \\ &\lesssim \text{tr} \left\{ \Sigma_{n,r,\lambda}^{-1} (\mathbb{E} \overline{R}_x^\top M_z \mathbb{E} \overline{R}_x / n) \Sigma_{n,r,\lambda}^{-1} \Sigma_{n,r,\lambda}^{-1} (\mathbb{E} \overline{R}_x^\top M_z \mathbb{E} \overline{R}_x / n) \Sigma_{n,r,\lambda}^{-1} \right\} \lesssim \frac{K}{(\nu_{KL} + \lambda \rho_D)^2} \end{aligned}$$

by (A.8). Further,

$$\begin{aligned} \left| \frac{1}{n} \sum_{i=1}^n \pi_{n,i,i} \varepsilon_i^2(s) - \mu_n \right| &= \left| \text{tr} \left\{ \Xi_n^\top \Phi_{\mathcal{I}} \Xi_n \left(Z^\top \left[\widetilde{\mathbf{V}}_n(s) - \mathbf{V}_n(s) \right] Z/n \right) \right\} \right| \\ &\leq \|\Xi_n^\top \Phi_{\mathcal{I}} \Xi_n\| \cdot \left\| Z^\top \left[\widetilde{\mathbf{V}}_n(s) - \mathbf{V}_n(s) \right] Z/n \right\| \end{aligned}$$

$$\lesssim_p \frac{L\sqrt{K}}{\sqrt{n}(\nu_{KL} + \lambda\rho_D)}$$

as in the proof of Theorem 3.2(iii), (iv).

Meanwhile, for a sufficiently large n ,

$$\begin{aligned} v_n &= 2\text{tr} \left\{ \Xi_n^\top \Phi_{\mathcal{I}} \Xi_n (Z^\top \mathbf{V}_n(s) Z/n) \Xi_n^\top \Phi_{\mathcal{I}} \Xi_n (Z^\top \mathbf{V}_n(s) Z/n) \right\} \\ &\geq c_1 \text{tr} \left\{ (Z^\top \mathbf{V}_n(s) Z/n) \Xi_n^\top \Xi_n (Z^\top \mathbf{V}_n(s) Z/n) \Xi_n^\top \Xi_n \right\} \\ &\geq c_2 \text{tr} \left\{ \Xi_n (Z^\top Z/n) \Xi_n^\top \Xi_n (Z^\top Z/n) \Xi_n^\top \right\} \\ &= c_2 \text{tr} \left\{ \Sigma_{n,r,\lambda}^{-1} (\mathbb{E} \bar{R}_x^\top M_z \mathbb{E} \bar{R}_x/n) \Sigma_{n,r,\lambda}^{-1} \Sigma_{n,r,\lambda}^{-1} (\mathbb{E} \bar{R}_x^\top M_z \mathbb{E} \bar{R}_x/n) \Sigma_{n,r,\lambda}^{-1} \right\} \\ &\geq \{c_3/(1+\lambda) - c_4\lambda/(\nu_{KL} + \lambda\rho_D)\}^2 K \\ &\geq c_5 K > 0 \end{aligned} \tag{A.12}$$

for some constants c_1, \dots, c_5 , by Assumptions 3.3(iii) and 3.7(ii) and (A.10). These imply that

$$\frac{\frac{1}{n} \sum_{i=1}^n \pi_{n,i,i} \varepsilon_i^2(s) - \mu_n}{\sqrt{v_n}} \lesssim_p \frac{L}{\sqrt{n}(\nu_{KL} + \lambda\rho_D)} \rightarrow 0.$$

Hence, we have

$$\frac{nB_{21}^\top \Phi_{\mathcal{I}} B_{21} - \mu_n}{\sqrt{v_n}} = \sum_{1 \leq i < j \leq n} \zeta_{n,i,j} + o_P(1),$$

where $\zeta_{n,i,j} := (n\sqrt{v_n})^{-1} 2\pi_{n,i,j} \varepsilon_i(s) \varepsilon_j(s)$.

To derive the limiting distribution of $\sum_{1 \leq i < j \leq n} \zeta_{n,i,j}$, we can use the central limit theorem for quadratic forms developed by de Jong (1987). From Proposition 3.2 of de Jong (1987), if (1) $\text{Var}(\sum_{1 \leq i < j \leq n} \zeta_{n,i,j}) = 1 + o(1)$, (2) $G_{n,I} = o(1)$, (3) $G_{n,II} = o(1)$, and (4) $G_{n,IV} = o(1)$, we have $\sum_{1 \leq i < j \leq n} \zeta_{n,i,j} \xrightarrow{d} N(0, 1)$, where

$$\begin{aligned} G_{n,I} &:= \sum_{1 \leq i < j \leq n} \mathbb{E}(\zeta_{n,i,j}^4) \\ G_{n,II} &:= \sum_{1 \leq i < j < k \leq n} \mathbb{E}(\zeta_{n,i,j}^2 \zeta_{n,i,k}^2 + \zeta_{n,j,i}^2 \zeta_{n,j,k}^2 + \zeta_{n,k,i}^2 \zeta_{n,k,j}^2) \\ G_{n,IV} &:= \sum_{1 \leq i < j < k < l \leq n} \mathbb{E}(\zeta_{n,i,j} \zeta_{n,i,k} \zeta_{n,l,j} \zeta_{n,l,k} + \zeta_{n,i,j} \zeta_{n,i,l} \zeta_{n,k,j} \zeta_{n,k,l} + \zeta_{n,i,k} \zeta_{n,i,l} \zeta_{n,j,k} \zeta_{n,j,l}). \end{aligned}$$

For (1), observe that

$$\begin{aligned} \text{Var} \left(\frac{2}{n} \sum_{1 \leq i < j \leq n} \pi_{n,i,j} \varepsilon_i(s) \varepsilon_j(s) \right) &= \frac{4}{n^2} \sum_{1 \leq i < j \leq n} \sum_{1 \leq k < l \leq n} \pi_{n,i,j} \pi_{n,k,l} \mathbb{E}[\varepsilon_i(s) \varepsilon_j(s) \varepsilon_k(s) \varepsilon_l(s)] \\ &= \frac{4}{n^2} \sum_{1 \leq i < j \leq n} \pi_{n,i,j}^2 \mathbb{E}[\varepsilon_i^2(s)] \mathbb{E}[\varepsilon_j^2(s)] \end{aligned}$$

$$\begin{aligned}
&= \frac{2}{n^2} \sum_{i \neq j} \text{tr} \{ \Xi_n^\top \Phi_{\mathcal{I}} \Xi_n z_j z_j^\top \Xi_n^\top \Phi_{\mathcal{I}} \Xi_n z_i z_i^\top \} \mathbb{E}[\varepsilon_i^2(s)] \mathbb{E}[\varepsilon_j^2(s)] \\
&= v_n - \frac{2}{n^2} \sum_{i=1}^n \text{tr} \{ \Xi_n^\top \Phi_{\mathcal{I}} \Xi_n z_i z_i^\top \Xi_n^\top \Phi_{\mathcal{I}} \Xi_n z_i z_i^\top \} (\mathbb{E}[\varepsilon_i^2(s)])^2.
\end{aligned}$$

By easy calculation, we can find

$$\frac{2}{n^2} \sum_{i=1}^n \text{tr} \{ \Xi_n^\top \Phi_{\mathcal{I}} \Xi_n z_i z_i^\top \Xi_n^\top \Phi_{\mathcal{I}} \Xi_n z_i z_i^\top \} (\mathbb{E}[\varepsilon_i^2(s)])^2 \lesssim \frac{KL}{n(\nu_{KL} + \lambda\rho_D)^2}.$$

Then, by (A.12), $\text{Var}(\sum_{1 \leq i < j \leq n} \zeta_{n,i,j}) \rightarrow 1$.

(2), (3), and (4) can be verified in the same manner as in the proof of Lemma A.11 of Hoshino (2022). Indeed, the following results hold:

$$\begin{aligned}
G_{n,I} &\lesssim L^3/(n^2 K^2 [\nu_{KL} + \lambda\rho_D]^4) + L^4/(n^3 K^2 [\nu_{KL} + \lambda\rho_D]^4) \\
G_{n,II} &\lesssim L^2/(n K^2 [\nu_{KL} + \lambda\rho_D]^4) + L^3/(n^2 K^2 [\nu_{KL} + \lambda\rho_D]^4) + L^4/(n^3 K^2 [\nu_{KL} + \lambda\rho_D]^4) \\
G_{n,IV} &\lesssim 1/(K [\nu_{KL} + \lambda\rho_D]^2) + L^4/(n K^2 [\nu_{KL} + \lambda\rho_D]^4) + L^4/(n^2 K^2 [\nu_{KL} + \lambda\rho_D]^4) - G_{n,II}.
\end{aligned}$$

This completes the proof. \square

Proof of Theorem 3.3

Our test statistic is defined as a standardization of $T_n = n \int_{\mathcal{I}} \widehat{\alpha}_n^2(t, s) dt$. Trivially, under \mathbb{H}_0 , we can write $T_n = n \int_{\mathcal{I}} (\widehat{\alpha}_n(t, s) - \alpha_0(t, s))^2 dt$. In view of (A.12), if we can verify that

$$T_n - n B_{21}^\top \Phi_{\mathcal{I}} B_{21} = o_P(\sqrt{K}),$$

the proof is completed by Lemma A.5.

Observe that

$$\begin{aligned}
T_n &= n \int_{\mathcal{I}} (\widehat{\alpha}_n(t, s) - \alpha_0(t, s))^2 dt \\
&= n \int_{\mathcal{I}} (\phi_K(t)^\top [\widehat{\theta}_n(s) - \theta_0(s)] + [\phi_K(t)^\top \theta_0(s) - \alpha_0(t, s)])^2 dt \\
&= n [\widehat{\theta}_n(s) - \theta_0(s)]^\top \Phi_{\mathcal{I}} [\widehat{\theta}_n(s) - \theta_0(s)] + 2n \int_{\mathcal{I}} \phi_K(t)^\top [\widehat{\theta}_n(s) - \theta_0(s)] [\phi_K(t)^\top \theta_0(s) - \alpha_0(t, s)] dt \\
&\quad + n \underbrace{\int_{\mathcal{I}} (\phi_K(t)^\top \theta_0(s) - \alpha_0(t, s))^2 dt}_{\leq \ell_K^2(s)}.
\end{aligned}$$

By Cauchy–Schwarz inequality,

$$\begin{aligned}
&\left| \int_{\mathcal{I}} \phi_K(t)^\top [\widehat{\theta}_n(s) - \theta_0(s)] [\phi_K(t)^\top \theta_0(s) - \alpha_0(t, s)] dt \right| \\
&\leq \ell_K(s) \left\| \phi_K(t)^\top [\widehat{\theta}_n(s) - \theta_0(s)] \right\|_{L^2} \lesssim_p \frac{\ell_K(s) \sqrt{K}}{\sqrt{n(\nu_{KL} + \lambda\rho_D)}} + \frac{\ell_K^2(s)}{\sqrt{\nu_{KL} + \lambda\rho_D}} + \frac{\lambda \ell_K(s) \|\theta_0(s)\|_D}{\nu_{KL} + \lambda\rho_D}
\end{aligned}$$

as in the proof of Theorem 3.1(ii).

Next, using the decomposition in the proof of Theorem 3.1(ii), write

$$n[\hat{\theta}_n(s) - \theta_0(s)]^\top \Phi_{\mathcal{I}}[\hat{\theta}_n(s) - \theta_0(s)] = n \sum_{a=1}^3 \sum_{b=1}^3 B_a^\top \Phi_{\mathcal{I}} B_b.$$

We can easily observe the following results:

$$|B_1^\top \Phi_{\mathcal{I}} B_1| \lesssim_p \frac{\lambda^2 \|\theta_0(s)\|_D^2}{(\nu_{KL} + \lambda\rho_D)^2}, \quad |B_3^\top \Phi_{\mathcal{I}} B_3| \lesssim_p \frac{\ell_K^2(s)}{\nu_{KL} + \lambda\rho_D}, \quad |B_1^\top \Phi_{\mathcal{I}} B_3| \lesssim_p \frac{\lambda \ell_K(s) \|\theta_0(s)\|_D}{(\nu_{KL} + \lambda\rho_D)^{3/2}}.$$

Moreover, write $B_1^\top \Phi_{\mathcal{I}} B_2 = B_1^\top \Phi_{\mathcal{I}} (B_{21} + B_{22} + B_{23})$. By similar calculations as above,

$$\begin{aligned} |B_1^\top \Phi_{\mathcal{I}} B_{21}| &= \lambda \left| \theta_0(s)^\top D \hat{\Sigma}_{n,r,\lambda}^{-1} \Phi_{\mathcal{I}} \Sigma_{n,r,\lambda}^{-1} \mathbb{E} \bar{R}_x^\top M_z \mathcal{E}(s) / n \right| \\ &\leq \lambda \left| \theta_0(s)^\top D \Sigma_{n,r,\lambda}^{-1} \Phi_{\mathcal{I}} \Sigma_{n,r,\lambda}^{-1} \mathbb{E} \bar{R}_x^\top M_z \mathcal{E}(s) / n \right| + \lambda \left| \theta_0(s)^\top D \left\{ \hat{\Sigma}_{n,r,\lambda}^{-1} - \Sigma_{n,r,\lambda}^{-1} \right\} \Phi_{\mathcal{I}} \Sigma_{n,r,\lambda}^{-1} \mathbb{E} \bar{R}_x^\top M_z \mathcal{E}(s) / n \right| \\ &\lesssim_p \frac{\lambda \|\theta_0(s)\|_D}{\sqrt{n}(\nu_{KL} + \lambda\rho_D)^{3/2}} + \frac{\lambda \|\theta_0(s)\|_D K \sqrt{L}}{n(\nu_{KL} + \lambda\rho_D)^{5/2}}. \end{aligned}$$

Similarly,

$$|B_1^\top \Phi_{\mathcal{I}} B_{22}| = \lambda \left| \theta_0(s)^\top D \hat{\Sigma}_{n,r,\lambda}^{-1} \Phi_{\mathcal{I}} \left\{ \hat{\Sigma}_{n,r,\lambda}^{-1} - \Sigma_{n,r,\lambda}^{-1} \right\} \mathbb{E} \bar{R}_x^\top M_z \mathcal{E}(s) / n \right| \lesssim_p \frac{\lambda \|\theta_0(s)\|_D K \sqrt{L}}{n(\nu_{KL} + \lambda\rho_D)^3}.$$

and

$$\begin{aligned} |B_1^\top \Phi_{\mathcal{I}} B_{23}| &= \lambda \left| \theta_0(s)^\top D \hat{\Sigma}_{n,r,\lambda}^{-1} \Phi_{\mathcal{I}} \hat{\Sigma}_{n,r,\lambda}^{-1} \left\{ (\bar{R}_x^\top Z / n) - \mathbb{E}(\bar{R}_x^\top Z / n) \right\}^\top (Z^\top Z / n)^{-1} Z^\top \mathcal{E}(s) / n \right| \\ &\lesssim_p \frac{\lambda \|\theta_0(s)\|_D L \sqrt{K}}{n(\nu_{KL} + \lambda\rho_D)^2}. \end{aligned}$$

We can also observe that

$$\begin{aligned} |B_3^\top \Phi_{\mathcal{I}} B_{21}| &\lesssim_p \frac{\ell_K(s)}{\sqrt{n}(\nu_{KL} + \lambda\rho_D)} + \frac{\ell_K(s) K \sqrt{L}}{n(\nu_{KL} + \lambda\rho_D)^{5/2}} + \frac{\ell_K(s) K \sqrt{L}}{n(\nu_{KL} + \lambda\rho_D)^{3/2}} \\ |B_3^\top \Phi_{\mathcal{I}} B_{22}| &\lesssim_p \frac{\ell_K(s) K \sqrt{L}}{n(\nu_{KL} + \lambda\rho_D)^{5/2}}, \quad |B_3^\top \Phi_{\mathcal{I}} B_{23}| \lesssim_p \frac{\ell_K(s) L \sqrt{K}}{n(\nu_{KL} + \lambda\rho_D)^{3/2}} \\ |B_{21}^\top \Phi_{\mathcal{I}} B_{22}| &\lesssim_p \frac{K \sqrt{KL}}{n^{3/2}(\nu_{KL} + \lambda\rho_D)^{5/2}}, \quad |B_{21}^\top \Phi_{\mathcal{I}} B_{23}| \lesssim_p \frac{KL}{n^{3/2}(\nu_{KL} + \lambda\rho_D)^{3/2}} \\ |B_{22}^\top \Phi_{\mathcal{I}} B_{22}| &\lesssim_p \frac{K^2 L}{n^2(\nu_{KL} + \lambda\rho_D)^4}, \quad |B_{23}^\top \Phi_{\mathcal{I}} B_{23}| \lesssim_p \frac{KL^2}{n^2(\nu_{KL} + \lambda\rho_D)^2}, \quad |B_{22}^\top \Phi_{\mathcal{I}} B_{23}| \lesssim_p \frac{(KL)^{3/2}}{n^2(\nu_{KL} + \lambda\rho_D)^3}. \end{aligned}$$

Under the assumptions made, we can find that $T_n = nB_{21}^\top \Phi_{\mathcal{I}} B_{21} + o_p(\sqrt{K})$, as desired. \square

Proof of Theorem 3.4

Observe that

$$\begin{aligned}
\widehat{Q}(s) &= W_n \int_0^1 Q(t) \alpha_0(t, s) dt + X \beta_0(s) + \mathcal{E}(s) + E(s) \\
&= W_n \int_0^1 \widehat{Q}(t) \alpha_0(t, s) dt - W_n \int_0^1 E(t) \alpha_0(t, s) dt + X \beta_0(s) + \mathcal{E}(s) + E(s) \\
&= \widehat{R} \theta_0(s) + X \beta_0(s) + \mathcal{E}(s) + E(s) - V(s) + \widehat{U}(s),
\end{aligned}$$

where $E = (e_1, \dots, e_n)^\top$, $e_i := \widehat{q}_i - q_i$, $V(s) = (v_1(s), \dots, v_n(s))^\top$, $v_i(s) := \sum_{j=1}^n w_{i,j} \int_0^1 e_j(t) \alpha_0(t, s) dt$, $\widehat{U}(s) = (\widehat{u}_1(s), \dots, \widehat{u}_n(s))^\top$, and $\widehat{u}_i(s) := \sum_{j=1}^n w_{i,j} \int_0^1 \widehat{q}_j(t) \alpha_0(t, s) dt - \widehat{r}_i^\top \theta_0$. As shown in (A.4), $|e_i| \lesssim \kappa^\xi$ uniformly. From this, $|v_i(s)| \lesssim \kappa^\xi$ is straightforward. Further, similar to (A.5), we have $|\widehat{u}_i(s)| \lesssim \ell_K(s)$ uniformly. Write

$$\begin{aligned}
\widetilde{\beta}_n(s) - \beta_0(s) &= \left[X^\top (I_n - \widehat{S}) X \right]^{-1} X^\top (I_n - \widehat{S}) \widehat{Q}(s) - \beta_0(s) \\
&= \left[X^\top (I_n - \widehat{S}) X \right]^{-1} X^\top (I_n - \widehat{S}) [\mathcal{E}(s) + \widehat{U}(s) + E(s) - V(s)] \\
&=: A'_1 + A'_2 + A'_3 + A'_4, \text{ say.}
\end{aligned}$$

Applying Fact A.2 in Hoshino (2022) and Lemmas A.3(ii) and A.4(iv), we have

$$\begin{aligned}
&\left\| X^\top \widehat{S} X/n - \mathbb{E}(X^\top \overline{R}/n) \left[\mathbb{E} \overline{R}^\top M_z \mathbb{E} \overline{R}/n \right]^{-1} \mathbb{E}(\overline{R}^\top X/n) \right\| \\
&\lesssim \rho_{\max} \left((\widehat{R}^\top X/n)(X^\top \widehat{R}/n) \right) \left\| \left[\widehat{R}^\top M_z \widehat{R}/n \right]^{-1} - \left[\mathbb{E} \overline{R}^\top M_z \mathbb{E} \overline{R}/n \right]^{-1} \right\| \\
&\quad + \rho_{\max} \left(\left[\mathbb{E} \overline{R}^\top M_z \mathbb{E} \overline{R}/n \right]^{-1} \right) \left\| \widehat{R}^\top X/n - \mathbb{E}(\overline{R}^\top X/n) \right\| \lesssim_p \frac{\sqrt{KL}}{\nu_{KL}^2 \sqrt{n}} + \frac{\kappa^\xi \sqrt{KL}}{\nu_{KL}^2} + \frac{\sqrt{K}}{\nu_{KL} \sqrt{n}} + \frac{\kappa^\xi \sqrt{K}}{\nu_{KL}}.
\end{aligned}$$

This implies that $\|X^\top (I_n - \widehat{S}) X/n - \Sigma_{n,x}\| \lesssim_p \sqrt{KL}/(\nu_{KL}^2 \sqrt{n})$ and that $\rho \left(X^\top (I_n - \widehat{S}) X/n \right) > 0$ with probability approaching one. Then, by the same argument as in the proof of Theorem 3.1(i), we can easily observe that $\|A'_2\| \lesssim_p \ell_K(s)$, $\|A'_3\| \lesssim_p \kappa^\xi$, and $\|A'_4\| \lesssim_p \kappa^\xi$ hold.

For A'_1 , decompose $A'_1 = A_1 + A'_{12} + A'_{13}$, where

$$\begin{aligned}
A_1 &= \left[X^\top (I_n - S) X/n \right]^{-1} X^\top (I_n - S) \mathcal{E}(s)/n \\
A'_{12} &= \left[X^\top (I_n - S) X/n \right]^{-1} X^\top (S - \widehat{S}) \mathcal{E}(s)/n \\
A'_{13} &= \left\{ \left[X^\top (I_n - \widehat{S}) X/n \right]^{-1} - \left[X^\top (I_n - S) X/n \right]^{-1} \right\} X^\top (I_n - \widehat{S}) \mathcal{E}(s)/n.
\end{aligned}$$

Write

$$\begin{aligned}
&X^\top (S - \widehat{S}) \mathcal{E}(s)/n \\
&= (X^\top Z/n)(Z^\top Z/n)^{-1} \underbrace{\left\{ (Z^\top \overline{R}/n) \left[\overline{R}^\top M_z \overline{R}/n \right]^{-1} (\overline{R}^\top Z/n) - (Z^\top \widehat{R}/n) \left[\widehat{R}^\top M_z \widehat{R}/n \right]^{-1} (\widehat{R}^\top Z/n) \right\}}_{=: L} (Z^\top Z/n)^{-1} Z^\top \mathcal{E}(s)/n.
\end{aligned}$$

By the same argument as above, we observe that

$$\begin{aligned} \|\mathbf{L}\| &\lesssim \rho_{\max} \left((\bar{\mathbf{R}}^\top Z/n)(Z^\top \bar{\mathbf{R}}/n) \right) \left\| [\bar{\mathbf{R}}^\top M_z \bar{\mathbf{R}}/n]^{-1} - [\hat{\mathbf{R}}^\top M_z \hat{\mathbf{R}}/n]^{-1} \right\| \\ &\quad + \rho_{\max} \left([\hat{\mathbf{R}}^\top M_z \hat{\mathbf{R}}/n]^{-1} \right) \left\| \bar{\mathbf{R}}^\top Z/n - \hat{\mathbf{R}}^\top Z/n \right\| \lesssim_p \frac{\kappa^\xi \sqrt{KL}}{\nu_{KL}^2} + \frac{\kappa^\xi \sqrt{KL}}{\nu_{KL}}. \end{aligned}$$

Thus,

$$\begin{aligned} \|A'_{12}\|^2 &= \mathcal{E}(s)^\top (S - \hat{S})X [X^\top (I_n - S)X/n]^{-2} X^\top (S - \hat{S})\mathcal{E}(s)/n^2 \\ &\lesssim_p (\mathcal{E}(s)^\top Z/n)(Z^\top Z/n)^{-1} \mathbf{L}(Z^\top Z/n)^{-1} (Z^\top X/n)(X^\top Z/n)(Z^\top Z/n)^{-1} \mathbf{L}(Z^\top Z/n)^{-1} (Z^\top \mathcal{E}(s)/n) \\ &\lesssim_p \|\mathbf{L}\|^2 \cdot \|Z^\top \mathcal{E}(s)/n\|^2, \end{aligned}$$

which yields $\|A'_{12}\| \lesssim_p \kappa^\xi L \sqrt{K}/(\sqrt{n}\nu_{KL}^2)$. Similarly,

$$\begin{aligned} \|A'_{13}\| &\lesssim_p \left\| [X^\top (I_n - \hat{S})X/n]^{-1} - [X^\top (I_n - S)X/n]^{-1} \right\| \\ &\quad \times \left\{ \|X^\top \mathcal{E}(s)/n\| + \|X^\top Z(Z^\top Z)^{-1} Z \hat{\mathbf{R}} [\hat{\mathbf{R}}^\top M_z \hat{\mathbf{R}}]^{-1} \hat{\mathbf{R}}^\top Z(Z^\top Z)^{-1} Z^\top \mathcal{E}(s)/n\| \right\} \\ &\lesssim_p \frac{\kappa^\xi \sqrt{KL}}{\sqrt{n}\nu_{KL}^2} + \frac{\kappa^\xi L \sqrt{K}}{\sqrt{n}\nu_{KL}^2}. \end{aligned}$$

Combining all these results, we have

$$\tilde{\beta}_n(s) - \beta_0(s) - A_1 \lesssim_p \frac{\kappa^\xi L \sqrt{K}}{\sqrt{n}\nu_{KL}^2} + \ell_K(s) + \kappa^\xi = o_P(n^{-1/2}),$$

which implies that $\tilde{\beta}_n(s)$ and $\hat{\beta}_n(s)$ have the same asymptotic distribution.

Next, similar to the above discussion, decompose

$$\begin{aligned} \tilde{\theta}_n(s) - \theta_0(s) &= \left[\hat{\mathbf{R}}_x^\top M_z \hat{\mathbf{R}}_x + \lambda Dn \right]^{-1} \hat{\mathbf{R}}_x^\top M_z \hat{\mathbf{Q}}(s) - \theta_0(s) \\ &= \left[\hat{\mathbf{R}}_x^\top M_z \hat{\mathbf{R}}_x + \lambda Dn \right]^{-1} \hat{\mathbf{R}}_x^\top M_z \hat{\mathbf{R}} \theta_0(s) - \theta_0(s) \\ &\quad + \left[\hat{\mathbf{R}}_x^\top M_z \hat{\mathbf{R}}_x + \lambda Dn \right]^{-1} \hat{\mathbf{R}}_x^\top M_z [\mathcal{E}(s) + \hat{\mathbf{U}}(s) + E(s) - V(s)] \\ &=: B'_1 + B'_2 + B'_3 + B'_4 + B'_5, \text{ say.} \end{aligned}$$

By Lemma A.4(iii), we have $\rho_{\max}([\hat{\mathbf{R}}_x^\top M_z \hat{\mathbf{R}}_x/n + \lambda D]^{-1}) \lesssim_p (\nu_{KL} + \lambda \rho_D)^{-1}$. Then, for B'_1 , noting that $B'_1 = -\lambda[\hat{\mathbf{R}}_x^\top M_z \hat{\mathbf{R}}_x/n + \lambda D]^{-1} D \theta_0(s)$, we have

$$\|B'_1\| \lesssim_p \frac{\lambda \|\theta_0(s)\|_D}{\nu_{KL} + \lambda \rho_D}.$$

Additionally, we can easily find that $\|B'_3\| \lesssim_p \ell_K(s)/\sqrt{\nu_{KL} + \lambda \rho_D}$, $\|B'_4\| \lesssim_p \kappa^\xi/\sqrt{\nu_{KL} + \lambda \rho_D}$, and $\|B'_5\| \lesssim_p \kappa^\xi/\sqrt{\nu_{KL} + \lambda \rho_D}$ hold.

For B'_2 , decompose it further as $B'_2 = B_2 + B'_{22} + B'_{23}$, where

$$\begin{aligned} B_2 &= \left[\bar{R}_x^\top M_z \bar{R}_x / n + \lambda D \right]^{-1} \bar{R}_x^\top M_z \mathcal{E}(s) / n \\ B'_{22} &= \left[\bar{R}_x^\top M_z \bar{R}_x / n + \lambda D \right]^{-1} (\hat{R}_x - \bar{R}_x)^\top M_z \mathcal{E}(s) / n \\ B'_{23} &= \left\{ \left[\hat{R}_x^\top M_z \hat{R}_x / n + \lambda D \right]^{-1} - \left[\bar{R}_x^\top M_z \bar{R}_x / n + \lambda D \right]^{-1} \right\} \hat{R}_x^\top M_z \mathcal{E}(s) / n. \end{aligned}$$

By Lemma A.3(ii), we have

$$\begin{aligned} \|B'_{22}\| &= \left\| \left[\bar{R}_x^\top M_z \bar{R}_x / n + \lambda D \right]^{-1} (\hat{R}Z/n - \bar{R}Z/n)^\top (Z^\top Z/n)^{-1} Z^\top \mathcal{E}(s) / n \right\| \\ &\quad + \left\| \left[\bar{R}_x^\top M_z \bar{R}_x / n + \lambda D \right]^{-1} (\hat{R}X/n - \bar{R}X/n)^\top (X^\top X/n)^{-1} X^\top \mathcal{E}(s) / n \right\| \\ &\lesssim_p \frac{\kappa^\xi L \sqrt{K}}{\sqrt{n}(\nu_{KL} + \lambda \rho_D)} + \frac{\kappa^\xi \sqrt{K}}{\sqrt{n}(\nu_{KL} + \lambda \rho_D)}. \end{aligned}$$

It also holds that

$$\begin{aligned} \|B'_{23}\| &\leq \left\| \left[\hat{R}_x^\top M_z \hat{R}_x / n + \lambda D \right]^{-1} - \left[\bar{R}_x^\top M_z \bar{R}_x / n + \lambda D \right]^{-1} \right\| \cdot \left\| \hat{R}_x^\top M_z \mathcal{E}(s) / n \right\| \\ &\lesssim_p \frac{\kappa^\xi L \sqrt{K}}{\sqrt{n}(\nu_{KL} + \lambda \rho_D)^2}. \end{aligned}$$

Hence, we have

$$\begin{aligned} &\frac{\sqrt{n}(\tilde{\alpha}_n(t, s) - \alpha_0(t, s) - \phi_K(t)^\top B_2)}{\sigma_{n,\lambda}(t, s)} \\ &= \frac{\sqrt{n} \phi_K(t)^\top (B'_1 + B'_{22} + B'_{23} + B'_3 + B'_4 + B'_5)}{\sigma_{n,\lambda}(t, s)} + \frac{\sqrt{n}(\phi_K(t)^\top \theta_0(s) - \alpha_0(t, s))}{\sigma_{n,\lambda}(t, s)} \\ &\lesssim_p \frac{\sqrt{n} \lambda \|\theta_0(s)\|_D}{\nu_{KL} + \lambda \rho_D} + \frac{\kappa^\xi L \sqrt{K}}{(\nu_{KL} + \lambda \rho_D)^2} + \frac{\sqrt{n}(\ell_K(s) + \kappa^\xi)}{\sqrt{\nu_{KL} + \lambda \rho_D}} + \frac{\sqrt{n} |\phi_K(t)^\top \theta_0(s) - \alpha_0(t, s)|}{\|\phi_K(t)\|} = o(1), \end{aligned}$$

implying the desired result.

B Supplementary simulation results

This section provides the detailed simulation results under incompletely observed outcome functions. As described in the main text, we suppose that for each unit i we can observe $\{(s_{i,j}, q_i(y_{i,j}))\}_{j=1}^m$, where $s_{i,j}$'s are uniformly randomly drawn from $[0, 1]$, for $m \in \{15, 50\}$. To recover the entire functional form of the q_i function, we apply the linear interpolation method in (3.2). The simulation scenarios examined are all identical to those used in the main text. The results for the 2SLS estimator and the Wald test are summarized in Tables B1 and B2, respectively.

Table B1: Estimation performance

DGP	m	n	# knots	β		$\alpha (\lambda_c = 0.5)$		$\alpha (\lambda_c = 1)$		$\alpha (\lambda_c = 2)$		$\alpha (\lambda_c = 3)$	
				BIAS	RMSE	BIAS	RMSE	BIAS	RMSE	BIAS	RMSE	BIAS	RMSE
1	15	400	2	0.0002	0.0376	0.0214	0.1071	0.0228	0.1036	0.0203	0.1022	0.0162	0.1010
			3	0.0004	0.0385	0.0221	0.1199	0.0230	0.1157	0.0197	0.1136	0.0149	0.1119
		1600	2	0.0008	0.0184	0.0161	0.0974	0.0201	0.0962	0.0223	0.0978	0.0220	0.0991
	50	400	3	0.0007	0.0184	0.0170	0.1118	0.0208	0.1097	0.0226	0.1105	0.0220	0.1112
			2	-0.0010	0.0370	0.0202	0.1060	0.0214	0.1025	0.0189	0.1010	0.0148	0.0997
		1600	2	-0.0008	0.0372	0.0208	0.1187	0.0217	0.1147	0.0184	0.1125	0.0136	0.1108
2	15	400	3	-0.0004	0.0176	0.0152	0.0959	0.0190	0.0951	0.0211	0.0968	0.0208	0.0980
			2	-0.0004	0.0177	0.0161	0.1102	0.0197	0.1086	0.0214	0.1094	0.0208	0.1102
		1600	2	-0.0001	0.0377	-0.0023	0.0917	-0.0065	0.0829	-0.0134	0.0769	-0.0196	0.0742
	50	400	3	0.0002	0.0388	-0.0023	0.1074	-0.0067	0.0990	-0.0143	0.0931	-0.0211	0.0903
			2	0.0007	0.0184	-0.0001	0.0848	-0.0024	0.0808	-0.0060	0.0774	-0.0091	0.0757
		1600	2	0.0007	0.0184	0.0001	0.1015	-0.0023	0.0976	-0.0061	0.0942	-0.0094	0.0925
3	15	400	3	-0.0012	0.0375	-0.0011	0.0921	-0.0055	0.0836	-0.0125	0.0775	-0.0188	0.0748
			2	-0.0012	0.0376	-0.0011	0.1078	-0.0058	0.0996	-0.0134	0.0937	-0.0203	0.0908
		1600	2	-0.0005	0.0179	0.0013	0.0851	-0.0012	0.0813	-0.0049	0.0780	-0.0081	0.0763
	50	400	3	-0.0005	0.0181	0.0014	0.1018	-0.0011	0.0981	-0.0051	0.0948	-0.0085	0.0930
			2	-0.0004	0.0401	0.0074	0.1841	0.0100	0.1964	0.0076	0.2076	0.0027	0.2125
		1600	2	-0.0004	0.0410	0.0079	0.1870	0.0099	0.2008	0.0065	0.2125	0.0008	0.2172
3	15	400	3	0.0007	0.0195	0.0006	0.1559	0.0061	0.1708	0.0096	0.1885	0.0098	0.1977
			2	0.0007	0.0197	0.0016	0.1552	0.0067	0.1732	0.0098	0.1927	0.0094	0.2024
		1600	2	-0.0014	0.0395	0.0142	0.1823	0.0171	0.1946	0.0148	0.2061	0.0100	0.2112
	50	400	3	-0.0014	0.0399	0.0148	0.1852	0.0170	0.1993	0.0138	0.2116	0.0081	0.2165
			2	-0.0005	0.0192	0.0071	0.1545	0.0127	0.1682	0.0165	0.1862	0.0168	0.1957
		1600	2	-0.0005	0.0192	0.0081	0.1533	0.0134	0.1707	0.0167	0.1907	0.0165	0.2009

C Supplementary material for the empirical analysis in Section 5

This section provides supplementary material for the empirical analysis. Table C3 presents the definitions of the variables used and their summary statistics. The estimated functional coefficients and the 95% confidence intervals are shown in Figure C1.

Table B2: Rejection frequency

n	# knots	m	λ_c	$\varrho = 0$			$\varrho = 0.1$			$\varrho = 0.2$			
				10%	5%	1%	10%	5%	1%	10%	5%	1%	
400	2	15	0.5	0.071	0.035	0.016	0.261	0.194	0.105	0.967	0.939	0.829	
			1	0.063	0.035	0.020	0.710	0.608	0.440	1.000	0.998	0.992	
			2	0.056	0.032	0.015	0.946	0.921	0.861	1.000	1.000	1.000	
		3	0.051	0.035	0.019	0.974	0.959	0.921	1.000	1.000	1.000		
		50	0.5	0.079	0.049	0.018	0.298	0.210	0.110	0.983	0.967	0.880	
			1	0.077	0.048	0.019	0.737	0.641	0.469	1.000	0.998	0.995	
			2	0.069	0.040	0.019	0.969	0.945	0.903	1.000	1.000	1.000	
		3	0.062	0.044	0.023	0.981	0.975	0.955	1.000	1.000	1.000		
		3	15	0.5	0.068	0.034	0.016	0.242	0.178	0.096	0.955	0.919	0.797
	1			0.060	0.034	0.016	0.690	0.590	0.430	1.000	0.998	0.991	
	2			0.052	0.031	0.013	0.941	0.912	0.844	1.000	1.000	1.000	
	3		0.045	0.033	0.016	0.964	0.950	0.917	1.000	1.000	1.000		
	50		0.5	0.073	0.046	0.018	0.292	0.205	0.105	0.980	0.959	0.872	
			1	0.072	0.044	0.018	0.741	0.650	0.479	1.000	0.999	0.995	
			2	0.061	0.036	0.017	0.965	0.941	0.901	1.000	1.000	1.000	
	3		0.061	0.041	0.023	0.979	0.970	0.955	1.000	1.000	1.000		
	1600		2	15	0.5	0.058	0.043	0.023	0.505	0.364	0.188	0.998	0.996
		1			0.057	0.043	0.023	0.936	0.875	0.692	1.000	1.000	0.999
2		0.063			0.040	0.022	0.997	0.997	0.990	1.000	1.000	1.000	
3		0.064		0.041	0.022	0.999	0.999	0.998	1.000	1.000	1.000		
50		0.5		0.078	0.054	0.028	0.611	0.449	0.243	1.000	1.000	1.000	
		1		0.078	0.053	0.029	0.970	0.942	0.791	1.000	1.000	1.000	
		2		0.077	0.052	0.028	1.000	1.000	0.998	1.000	1.000	1.000	
3		0.078		0.052	0.026	1.000	1.000	1.000	1.000	1.000	1.000		
3		15		0.5	0.056	0.041	0.023	0.501	0.353	0.176	0.999	0.996	0.990
			1	0.055	0.041	0.022	0.940	0.869	0.695	1.000	1.000	0.999	
			2	0.062	0.039	0.021	0.998	0.997	0.990	1.000	1.000	1.000	
		3	0.061	0.040	0.020	1.000	0.999	0.998	1.000	1.000	1.000		
		50	0.5	0.074	0.051	0.027	0.605	0.439	0.236	1.000	1.000	1.000	
			1	0.074	0.050	0.028	0.972	0.942	0.808	1.000	1.000	1.000	
			2	0.076	0.050	0.028	1.000	1.000	0.999	1.000	1.000	1.000	
		3	0.077	0.049	0.026	1.000	1.000	1.000	1.000	1.000	1.000		

Table C3: Descriptive statistics ($n = 1883$)

Variable	Mean	Std. Dev.	Min.	Max.
Landprice	10.083	1.191	7.313	14.883
Unemployment	3.687	1.134	0	10.635
Agriculture	0.078	0.081	0	0.467
Sales	10.500	2.196	0	17.666
Beds	1.089	1.051	0	13.489
Childcare	0.290	0.209	0.000	2.833
$q(0.25)$	31.801	5.638	17.904	58.162
$q(0.5)$	52.777	5.865	38.113	71.003
$q(0.75)$	69.895	3.877	54.193	99.028

Definitions: Landprice = $\log(\text{average residential landprice (JPY/m}^2\text{)})$; Unemployment = unemployment rate (%); Agriculture = proportion of agriculture, forestry, and fishery workers; Sales = $\log(\text{annual commercial sales (million JPY)} + 1)$; Beds = $100 \times \#$ of hospital beds/population; Childcare = $1000 \times \#$ of childcare facilities/population.

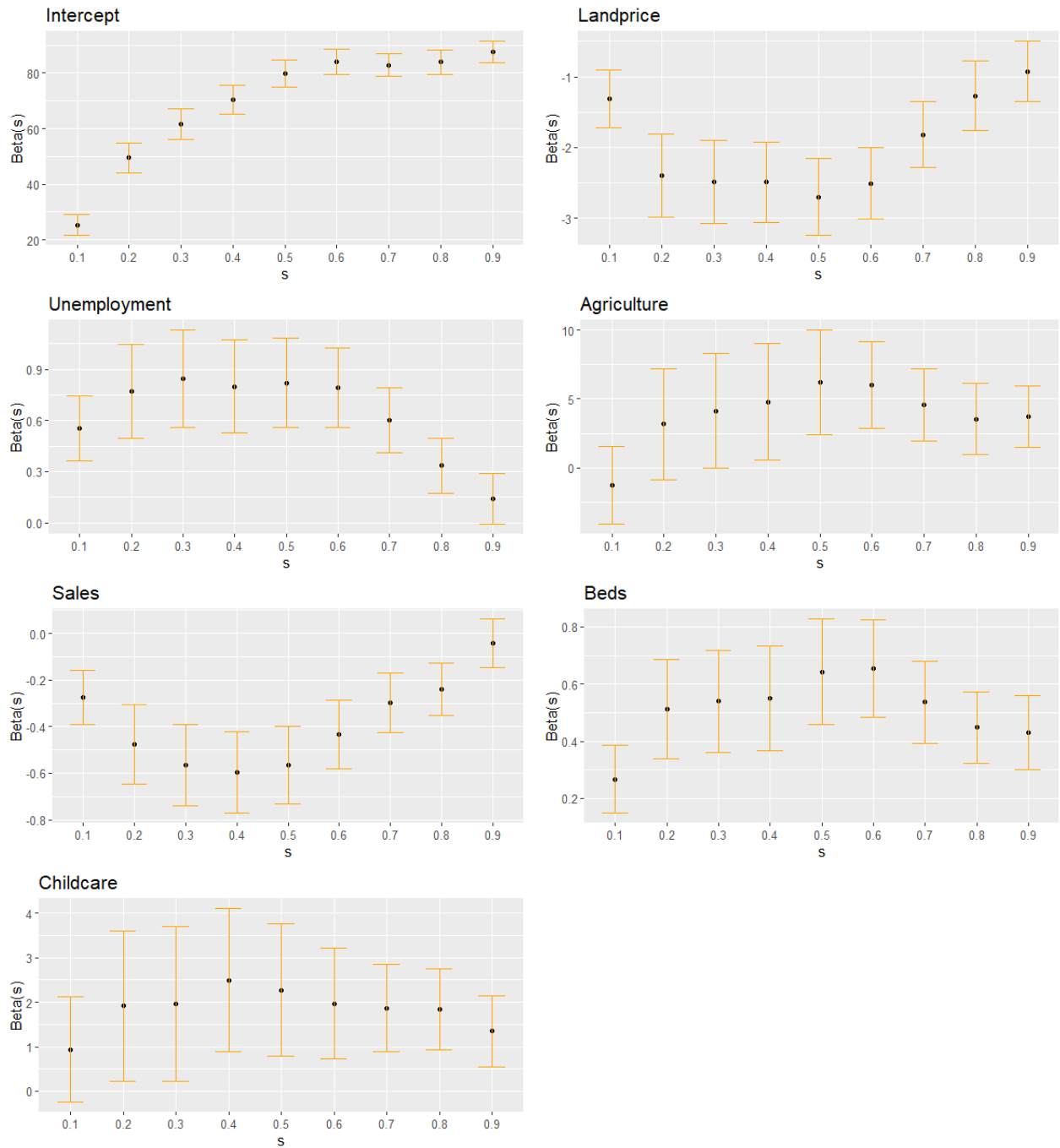


Figure C1: Estimated coefficients